Conservative high order positivity-preserving discontinuous Galerkin methods for linear hyperbolic and radiative transfer equations

Dan Ling[1], Juan Cheng[2], Chi-Wang Shu[3]

Abstract

We further investigate the high order positivity-preserving discontinuous Galerkin (DG) methods for linear hyperbolic and radiative transfer equations developed in [14]. The DG methods in [14] can maintain positivity and high order accuracy, but they rely both on the scaling limiter in [15] and a rotational limiter, the latter may alter cell averages of the unmodulated DG scheme, thereby affecting conservation. Even though a Lax-Wendroff type theorem is proved in [14], guaranteeing convergence to weak solutions with correct shock speed when such rotational limiter is applied, it would still be desirable if a conservative DG method without changing the cell averages can be obtained which has both high order accuracy and positivity-preserving capability. In this paper, we develop and analyze such a DG method for both linear hyperbolic equations and radiative transfer equations. In the one-dimensional case, the method uses traditional DG space P^k of piecewise polynomials of degree at most k. A key result is proved that the unmodulated DG solver in this case can maintain positivity of the cell average if the inflow boundary value and the source term are both positive, therefore the positivity-preserving framework in [15] can be used to obtain a high order conservative positivity-preserving DG scheme. Unfortunately, in two-dimensions this is no longer the case. We show that the unmodulated DG solver based either on P^k or Q^k spaces (piecewise k-th degree polynomials or piecewise tensor-product k-th degree polynomials) could generate negative cell averages. We augment the DG space with additional functions so that the positivity of cell averages from the unmodulated DG solver can be restored, thereby leading to high order conservative positivity-preserving DG scheme based on these augmented DG spaces following the framework in [15]. Computational results are provided to demonstrate the good performance of our DG schemes.

Keywords: Positivity-preserving; discontinuous Galerkin method; conservative schemes; linear hyperbolic equation; radiative transfer equation; high order accuracy.

[1]Graduate School, China Academy of Engineering Physics, Beijing 100088, China. E-mail: lingdan189@126.com.

[2]Institute of Applied Physics and Computational Mathematics, Beijing 100088, China. E-mail: cheng_juan@iapcm.ac.cn. Research is supported in part by NSFC grant 11471049 and U1630247 and Science Challenge Project. No. JCKY2016212A502.

[3]Division of Applied Mathematics, Brown University, Providence, RI 02912. E-mail: shu@dam.brown.edu. Research is supported in part by ARO grant W911NF-15-1-0226 and NSF grant DMS-1719410.

1 Introduction

We are concerned with the numerical solutions of linear hyperbolic conservation laws (both steady state and time dependent), and radiative transfer equations. These are the types of equations for which the very first discontinuous Galerkin (DG) method was designed, in [11]. In particular, we are concerned with the positivity-preserving property of the high order DG methods for such equations. This paper improves the results in [14], in a crucial way by obtaining conservative methods in the sense that the cell averages obtained by the unmodulated high order DG solver are not altered. We refer to [14] and the references therein for a detailed discussion on the background of the equations and the DG numerical methods used in this paper, and will only give a sketchy description before proceeding directly to the main new ideas in this paper.

Radiative transfer is the process of energy transfer in the form of electromagnetic radiation. Radiation passes through a medium affected by absorption, emission, and scattering procedures. The equation of radiative transfer describes these interactions mathematically. Equations of radiative transfer have applications in a wide variety of subjects including inertial confinement fusion, astrophysics, optical molecular imaging, shielding, atmospheric science, and remote sensing.

The radiative transfer equation is an integro-differential equation. The presence of integral coupling terms makes it more challenging to solve the equation numerically, especially for high dimensional cases. Several techniques for solving this kind of equations have been studied in recent literature, including the Monte Carlo method, the discrete-ordinate method (DOM), the spherical harmonics method, the spectral method, the finite difference method, the finite volume method, and the finite element method. We will pay attention in this paper only to the DOM [1, 6, 7] due to its relatively high accuracy, flexibility, and relatively low computational cost. By means of the DOM method, the solid angle appearing in the radiative transfer equation is discretized as a set of ordinate directions (numerical quadrature in the angular direction). The angle-discretized radiative transfer equation is then a system of

linear hyperbolic equations coupled through the source terms.

The DG method was first proposed and analyzed in the early 1970s exactly for this type of linear hyperbolic equations. In 1973, Reed and Hill introduced a DG method to solve the hyperbolic neutron transport equation (radiative transfer) [11]. Immediately after that, theoretical properties of this DG method including stability and error estimates were given in [8]. Later, Cockburn et al. [4, 3, 2, 5] established a framework to easily solve nonlinear time-dependent problems, such as the compressible Euler equations of gas dynamics, using explicit, nonlinearly stable high order Runge-Kutta time discretization [13] and DG discretization in space with exact or approximate Riemann solvers as interface fluxes and total variation bounded (TVB) nonlinear limiters [12] to achieve non-oscillatory properties for strong shocks. The DG method has many advantages such as high order accuracy, geometric flexibility, suitability for h- and p-adaptivity, extremely local data structure, high parallel efficiency and a good theoretical foundation for stability and error estimates.

When the DG method is used to solve the coupled system of linear hyperbolic equations with source terms arising from DOM, several difficulties arise due to the coupling. Usually, a source iteration technique is applied to "decouple" this system in each iteration, thus achieving a class of scalar equations in each iteration with the coupling deferred to the previous iteration, thereby amendable to the original sweeping DG method. This source iteration could be slow in the diffusive limit, but we are not going to discuss this difficulty in this paper.

The focus of this paper is on the positivity-preserving property of the high order DG solution. Physically and mathematically, the solution to the radiative transfer equation is positive (non-negative), however this property is often lost in numerical approximations, especially for high order methods. In [14], a high order positivity-preserving DG method is designed for linear hyperbolic equations and the source iteration of DOM for the radiative transfer equation. The crucial observation is the proof that, for the unmodulated DG scheme, the point value of the numerical solution at one particular point inside the cell remains

positive. Even though the exact location of this point is usually not known, it does not prevent the design of a positivity-preserving limiter, which is a combination of the scaling limiter designed in [15] when the cell average is positive, and a new rotational limiter used when the cell average is negative. It is proved in [14] that the usage of this rotational limiter does not affect the original high order accuracy of the DG scheme, nor does it affect convergence to weak solutions (correct shock speed, a Lax-Wendroff type theorem), even though conservation is lost when the original cell averages are altered through the rotational limiter. However, conservation (in the sense that the cell average from the unmodulated DG solver is not altered in the limiting process) is often treated as a sacred property, not to be lost at any cost. This is the motivation that we attempt to obtain high order positivity-preserving DG methods in this paper which are conservative, in the sense that the cell average from the unmodulated DG solver is never altered.

In the one-dimensional case, we prove a key result that the unmodulated DG solver, based on the standard DG space P^k of piecewise polynomials of degree at most k, can maintain positivity of the cell average when the inflow boundary value and the source term are both positive, therefore the positivity-preserving framework in [15] can be used to obtain a high order conservative positivity-preserving DG scheme. Unfortunately, in two-dimensions this is no longer the case. We show that the unmodulated DG solver based either on the P^k or Q^k spaces (piecewise k-th degree polynomials or piecewise tensor-product k-th degree polynomials) could generate negative cell averages. We then augment the DG space with additional functions so that the positivity of cell averages from the unmodulated DG solver can be restored, thereby leading to high order conservative positivity-preserving DG scheme based on these augmented DG spaces following the framework in [15].

The remainder of this paper is organized as follows: In Section 2, we first introduce the linear hyperbolic equations and the discrete-ordinate radiative transfer equations, and then formulate the DG discretization and implicit time discretization (for the time-dependent problems) for these equations both in one and two dimensional spaces. Section 3 considers

positivity-preserving DG scheme in one dimension. The proof that the cell averages of the unmodulated DG method remain positive and the development of the positivity-preserving method via the scaling limiter in [15] will be given. In Section 4, we first demonstrate the failure of cell average positivity from unmodulated DG methods based on either P^k or Q^k spaces, and then construct augmented DG spaces for the second order case as an example to restore this positivity, leading to the final development of the positivity-preserving DG method based on these augmented DG spaces via the scaling limiter in [15]. Finally, in Section 5, one- and two-dimensional numerical examples for solving linear hyperbolic equations and the source iteration of DOM from the radiative transfer equation will be given to verify the good performance of our positivity-preserving DG methods. Concluding remarks are given in Section 6.

2 The linear hyperbolic equation and the radiative transfer equation and their DG disretizations

2.1 The linear hyperbolic equation and its DG discretization in one spatial dimension

We consider the following linear steady hyperbolic equation,

$$\alpha u'(x) + \gamma u(x) = f(x), \tag{2.1}$$

where α and $\gamma \geq 0$ are constants and $f(x) \geq 0$ is the source term. Without loss of generality we assume $\alpha > 0$, in this case the boundary condition is given at the left boundary for the existence and uniqueness of the solution.

We denote $S_i = [x_{i-\frac{1}{2}}, x_{i+\frac{1}{2}}],\ i = 1, \ldots, N$ as a subdivision of the interval $[a, b]$ with

$$a = x_{\frac{1}{2}} < x_{\frac{3}{2}} < \cdots < x_{N+\frac{1}{2}} = b, \quad \Delta x_i = x_{i+\frac{1}{2}} - x_{i-\frac{1}{2}},$$

and $h = \max\limits_{1 \leq i \leq N} \Delta x_i$. The finite element space consists of the following piecewise polynomials

$$V_h^k = \left\{ v \in L^2(a, b) : v|_{S_i} \in P^k(S_i), \forall i = 1, \ldots, N \right\},$$

where $P^k(S_i)$ stands for the set of polynomials of degree up to k defined in the cell S_i.

The DG scheme for (2.1) is to seek the polynomial approximation $u_h(x) \in V_h^k$, such that for any $v(x) \in V_h^k$, there always holds

$$-\alpha \int_{S_i} u_h(x)v'(x)dx + \alpha \hat{u}_{i+\frac{1}{2}} v(x_{i+\frac{1}{2}}^-) + \gamma \int_{S_i} u_h(x)v(x)dx = \alpha \hat{u}_{i-\frac{1}{2}} v(x_{i-\frac{1}{2}}^+) + \int_{S_i} f(x)v(x)dx, \tag{2.2}$$

where $\hat{u}_{i\pm\frac{1}{2}}$ is the numerical flux. For the scheme (2.2) to be locally solvable (sweeping from the boundary), the numerical flux $\hat{u}_{i\pm\frac{1}{2}}$ at the cell interfaces must be chosen to be the upwind flux, that is

$$\hat{u}_{i+\frac{1}{2}} = u_h(x_{i+\frac{1}{2}}^-), \quad \hat{u}_{i-\frac{1}{2}} = u_h(x_{i-\frac{1}{2}}^-).$$

For simplicity, in the following, we denote $u_{i\pm\frac{1}{2}}^- = u_h(x_{i\pm\frac{1}{2}}^-)$, and $\overline{u}_i = \frac{1}{\Delta x_i}\int_{S_i} u_h(x)dx$ as the cell average of $u_h(x)$ in the interval S_i. We also omit the subscript h below.

For a time-dependent problem, the above linear hyperbolic equation becomes

$$\frac{\partial u(x,t)}{\partial t} + \alpha \frac{\partial u(x,t)}{\partial x} + \gamma u(x,t) = f(x,t), \quad \gamma \geq 0, \quad f \geq 0. \tag{2.3}$$

The semi-discrete DG scheme for (2.3) is to seek the polynomial approximation $u(\cdot,t) \in V_h^k$, such that for any $v(x) \in V_h^k$, there always holds

$$\begin{aligned} &\frac{d}{dt}\int_{S_i} u(x,t)v(x)dx - \alpha \int_{S_i} u(x,t)v'(x)dx + \alpha u_{i+\frac{1}{2}}^-(t)v_{i+\frac{1}{2}}^- + \gamma \int_{S_i} u(x,t)v(x)dx \\ &= \int_{S_i} f(x,t)v(x)dx + \alpha u_{i-\frac{1}{2}}^-(t)v_{i-\frac{1}{2}}^+. \end{aligned} \tag{2.4}$$

In this paper, we use the backward Euler method as the time discretization for all time-dependent problems. Assume that the approximation at time level n is denoted by $u^n(x) \in V_h^k$, then the fully discrete DG method for the equation in (2.4) can be described as follows: Find $u^{n+1}(x) \in V_h^k$ such that $\forall v(x) \in V_h^k$ we have

$$\begin{aligned} &\int_{S_i} u^{n+1}(x)v(x)dx - \alpha\Delta t^n \int_{S_i} u^{n+1}(x)v'(x)dx + \gamma\Delta t^n \int_{S_i} u^{n+1}(x)v(x)dx + \alpha\Delta t^n (u_{i+\frac{1}{2}}^{n+1})^- v_{i+\frac{1}{2}}^- \\ =&\Delta t^n \int_{S_i} f^{n+1}(x)v(x)dx + \int_{S_i} u^n(x)v(x)dx + \alpha\Delta t^n (u_{i-\frac{1}{2}}^{n+1})^- v_{i-\frac{1}{2}}^+, \end{aligned} \tag{2.5}$$

where Δt^n is the time step. Since the n-th time step solution $u_i^n(x)$ is known, (2.5) can be rewritten as

$$-\alpha \int_{S_i} u^{n+1}(x)v'(x)dx+\alpha(u_{i+\frac{1}{2}}^{n+1})^- v_{i+\frac{1}{2}}^- +\widetilde{\gamma} \int_{S_i} u^{n+1}(x)v(x)dx = \int_{S_i} \widetilde{f}(x)v(x)dx+\alpha(u_{i-\frac{1}{2}}^{n+1})^- v_{i-\frac{1}{2}}^+, \tag{2.6}$$

where $\widetilde{\gamma} = \gamma + \frac{1}{\Delta t^n}$ and $\widetilde{f}(x) = f^{n+1}(x) + \frac{1}{\Delta t^n} u^n(x)$. We notice that the scheme (2.6) is identical to (2.2) for solving the steady equation, therefore we only need to consider (2.2) below.

2.2 The linear hyperbolic equation and its DG discretization in two spatial dimensions

For the two-dimensional steady case, the linear hyperbolic equation we consider has the following general form

$$\alpha \frac{\partial u(x,y)}{\partial x} + \beta \frac{\partial u(x,y)}{\partial y} + \gamma u(x,y) = f(x,y), \quad \gamma \geq 0, \tag{2.7}$$

where α, β are constants and $f(x,y) \geq 0$ is the source term. We again assume $\alpha, \beta > 0$ without loss of generality. In this case the boundary condition is given at the left and bottom boundaries.

We denote the computational domain as $\mathcal{D} = [a,b] \times [c,d]$, which is divided into the rectangular mesh of $S_{i,j} = [x_{i-\frac{1}{2}}, x_{i+\frac{1}{2}}] \times [y_{j-\frac{1}{2}}, y_{j+\frac{1}{2}}]$ with $i = 1, \ldots, N_x, j = 1, \ldots, N_y$. The inflow boundary $\partial S_{i,j}^- = \Gamma_{in1} \cup \Gamma_{in2}$ and the outflow boundary $\partial S_{i,j}^+ = \Gamma_{out1} \cup \Gamma_{out2}$ can be described as follows:

$$\begin{array}{ll} \Gamma_{in1} = \{x_{i-\frac{1}{2}}\} \times [y_{j-\frac{1}{2}}, y_{j+\frac{1}{2}}], & \Gamma_{in2} = [x_{i-\frac{1}{2}}, x_{i+\frac{1}{2}}] \times \{y_{j-\frac{1}{2}}\}, \\ \Gamma_{out1} = \{x_{i+\frac{1}{2}}\} \times [y_{j-\frac{1}{2}}, y_{j+\frac{1}{2}}], & \Gamma_{out2} = [x_{i-\frac{1}{2}}, x_{i+\frac{1}{2}}] \times \{y_{j+\frac{1}{2}}\}. \end{array}$$

Now, let V_h^k be the finite element space, then the DG scheme for solving (2.7) can be described as: Find $u(x,y) \in V_h^k$ such that $\forall v(x,y) \in V_h^k$ we have

$$
\begin{aligned}
&-\int_{S_{i,j}} u(x,y)(\alpha v_x(x,y)+\beta v_y(x,y))dxdy+\alpha\int_{y_{j-\frac{1}{2}}}^{y_{j+\frac{1}{2}}} u(x^-_{i+\frac{1}{2}},y)v(x^-_{i+\frac{1}{2}},y)dy\\
&+\beta\int_{x_{i-\frac{1}{2}}}^{x_{i+\frac{1}{2}}} u(x,y^-_{j+\frac{1}{2}})v(x,y^-_{j+\frac{1}{2}})dx+\gamma\int_{S_{i,j}} u(x,y)v(x,y)dxdy\\
=&\int_{S_{i,j}} f(x,y)v(x,y)dxdy+\alpha\int_{y_{j-\frac{1}{2}}}^{y_{j+\frac{1}{2}}} u(x^-_{i-\frac{1}{2}},y)v(x^+_{i-\frac{1}{2}},y)dy+\beta\int_{x_{i-\frac{1}{2}}}^{x_{i+\frac{1}{2}}} u(x,y^-_{j-\frac{1}{2}})v(x,y^+_{j-\frac{1}{2}})dx.
\end{aligned}
\tag{2.8}
$$

Similarly, if we consider a time-dependent problem formulated as

$$
\frac{\partial u(x,y,t)}{\partial t}+\alpha\frac{\partial u(x,y,t)}{\partial x}+\beta\frac{\partial u(x,y,t)}{\partial y}+\gamma u(x,y,t)=f(x,y,t),\quad \gamma\geq 0,\quad f\geq 0, \tag{2.9}
$$

we obtain the corresponding DG scheme for (2.9) by means of backward Euler method for time discretization as follows

$$
\begin{aligned}
&-\int_{S_{i,j}} u^{n+1}(x,y)(\alpha v_x(x,y)+\beta v_y(x,y))dxdy+\alpha\int_{y_{j-\frac{1}{2}}}^{y_{j+\frac{1}{2}}} u^{n+1}(x^-_{i+\frac{1}{2}},y)v(x^-_{i+\frac{1}{2}},y)dy\\
&+\beta\int_{x_{i-\frac{1}{2}}}^{x_{i+\frac{1}{2}}} u^{n+1}(x,y^-_{j+\frac{1}{2}})v(x,y^-_{j+\frac{1}{2}})dx+\widetilde{\gamma}\int_{S_{i,j}} u^{n+1}(x,y)v(x,y)dxdy\\
=\;&\alpha\int_{y_{j-\frac{1}{2}}}^{y_{j+\frac{1}{2}}} u^{n+1}(x^-_{i-\frac{1}{2}},y)v(x^+_{i-\frac{1}{2}},y)dy+\beta\int_{x_{i-\frac{1}{2}}}^{x_{i+\frac{1}{2}}} u^{n+1}(x,y^-_{j-\frac{1}{2}})v(x,y^+_{j-\frac{1}{2}})dx\\
&+\int_{S_{i,j}}\widetilde{f}(x,y)v(x,y)dxdy,
\end{aligned}
\tag{2.10}
$$

where $\widetilde{\gamma}=\gamma+\frac{1}{\Delta t^n}$ and $\widetilde{f}(x,y)=f^{n+1}(x,y)+\frac{1}{\Delta t^n}u^n(x,y)$. We again notice that the scheme (2.10) is identical to (2.8) for solving the steady equation, therefore we only need to consider (2.8) below.

2.3 The radiative transfer equation and its DG discretization in one spatial dimension

The steady radiative transfer equation in one-dimensional planar geometry can be formulated as

$$
\mu\frac{\partial I(x,\mu)}{\partial x}+\sigma_t I(x,\mu)=\frac{\sigma_s}{2}\int_{-1}^{1} I(x,\mu)d\mu+q(x,\mu),\quad a\leq x\leq b,-1\leq\mu\leq 1, \tag{2.11}
$$

where $I(x,\mu)$ is the radiative intensity in the direction μ, σ_t is the extinction coefficient of the medium due to both absorption and scattering, $\sigma_s \geq 0$ is the scattering coefficient of the medium, i.e. $\sigma_s \leq \sigma_t$, and $q(x,\mu)$ is the source term. The boundary condition for (2.11) is given as follows:

$$I(a,\mu) = g_1(\mu),\ 0 < \mu \leq 1; \quad I(b,\mu) = g_2(\mu),\ \ -1 \leq \mu < 0. \tag{2.12}$$

By means of the discrete ordinate method (DOM) in [7], we can obtain the following spatial differential equation for each discrete direction m

$$\mu_m \frac{\partial I_m(x)}{\partial x} + \sigma_t I_m(x) = \frac{\sigma_s}{2} \sum_{m'=1}^{M} \omega_{m'} I_{m'}(x) + q_m(x), \quad m = 1, \ldots, M, \tag{2.13}$$

where μ_m is the direction cosines along the x-coordinate of the direction m, $\omega_m > 0$ is the quadrature weight with $\sum\limits_{m=1}^{M} \omega_m = 2$ and $I_m(x) = I(x,\mu_m)$ is the radiative intensity in the direction m.

Now, we also consider a given direction $\mu_m > 0$, as the case of $\mu_m < 0$ is similar. Then the DG method for solving (2.13) is described as follows: find $I_m(x) \in V_h^k$ such that for any test function $v(x) \in V_h^k$, we have

$$\begin{aligned} &-\mu_m \int_{S_i} I_m(x) v'(x) dx + \sigma_t \int_{S_i} I_m(x) v(x) dx + \mu_m I_m(x_{i+\frac{1}{2}}^-) v(x_{i+\frac{1}{2}}^-) \\ =&\frac{\sigma_s}{2} \int_{S_i} \varphi(x) v(x) dx + \int_{S_i} q_m(x) v(x) dx + \mu_m I_m(x_{i-\frac{1}{2}}^-) v(x_{i-\frac{1}{2}}^+), \end{aligned} \tag{2.14}$$

where

$$\varphi(x) = \sum_{m'=1}^{M} \omega_{m'} I_{m'}(x).$$

When considering the time-dependent problem, the unsteady radiative transfer equation in planar geometry is described as

$$\frac{1}{c} \frac{\partial I(x,\mu,t)}{\partial t} + \mu \frac{\partial I(x,\mu,t)}{\partial x} + \sigma_t I(x,\mu,t) = \frac{\sigma_s}{2} \int_{-1}^{1} I(x,\mu,t) d\mu + q(x,\mu,t), \tag{2.15}$$

where $a \leq x \leq b, -1 \leq \mu \leq 1, 0 < t \leq T$ and c is the speed of photon. The specific boundary

conditions and initial condition can be given as

$$\begin{aligned} I(a,\mu,t) &= I^l(\mu,t), \quad 0<\mu\le 1, 0\le t\le T; \\ I(b,\mu,t) &= I^r(\mu,t), \quad -1\le\mu<0, 0\le t\le T; \\ I(x,\mu,0) &= I_0(x,\mu). \end{aligned} \tag{2.16}$$

Likewise, the approximation obtained by using the DOM for (2.15) can be written as

$$\frac{1}{c}\frac{\partial I_m(x,t)}{\partial t}+\mu_m\frac{\partial I_m(x,t)}{\partial x}+\sigma_t I_m(x,t)=\frac{\sigma_s}{2}\sum_{m'=1}^{M}\omega_{m'}I_{m'}(x,t)+q_m(x,t), m=1,\ldots,M. \tag{2.17}$$

Making use of backward Euler time discretization for solving (2.17), we get the following DG scheme

$$\begin{aligned} &-\mu_m\int_{S_i} I_m^{n+1}(x)v'(x)dx+\widetilde{\sigma}_t\int_{S_i} I_m^{n+1}(x)v(x)dx+\mu_m I_m^{n+1}(x_{i+\frac{1}{2}}^-)v(x_{i+\frac{1}{2}}^-) \\ =&\frac{\sigma_s}{2}\int_{S_i}\varphi^{n+1}(x)v(x)dx+\int_{S_i}\widetilde{q}_m(x)v(x)dx+\mu_m I_m^{n+1}(x_{i-\frac{1}{2}}^-)v(x_{i-\frac{1}{2}}^+), \end{aligned} \tag{2.18}$$

where $\widetilde{\sigma}_t=\sigma_t+\frac{1}{c\Delta t^n}$ and $\widetilde{q}_m(x)=q_m^{n+1}(x)+\frac{1}{c\Delta t^n}I_m^n(x)$. This is now the same as the steady case (2.14).

Generally, the discrete set of algebraic equations in the DOM-DG schemes such as (2.14) and (2.18) is solved by the source iteration (SI) method [9] in an optimal sweeping order, which is usually referred to as the grid sweeping algorithm. More details can be found in [14]. Specifically, the SI method is defined for solving the DG scheme (2.14) as follows: When the ℓ-th iteration solution $I_m^{(\ell)}$ (for all $m=1,\ldots,M$ and all cells) is known, we compute $I_m^{(\ell+1)}$ cell by cell in the sweeping direction, and for each fixed cell, running through $m=1,\ldots,M$ to solve

$$\begin{aligned} &-\mu_m\int_{S_i} I_m^{(\ell+1)}(x)v'(x)dx+\sigma_t\int_{S_i} I_m^{(\ell+1)}(x)v(x)dx+\mu_m I_m^{(\ell+1)}(x_{i+\frac{1}{2}}^-)v(x_{i+\frac{1}{2}}^-) \\ =&\frac{\sigma_s}{2}\int_{S_i}\varphi^{(*)}(x)v(x)dx+\int_{S_i}q_m(x)v(x)dx+\mu_m I_m^{(\ell+1)}(x_{i-\frac{1}{2}}^-)v(x_{i-\frac{1}{2}}^+), \end{aligned} \tag{2.19}$$

with

$$\varphi^{(*)}(x)=\sum_{m'=1}^{M}\omega_{m'}I_{m'}^{(*)}(x),$$

where $I_{m'}^{(*)}(x)$ is taken as $I_{m'}^{(\ell+1)}(x)$ if it is already available; otherwise it is taken as $I_{m'}^{(\ell)}(x)$. Since $I_m^{(\ell+1)}(x_{i-\frac{1}{2}}^-)$ (for $i=1$ this is taken as the given boundary condition) and the other $(\ell+1)$-th iteration solution needed on the right-hand side of (2.19) have already been computed in the sweep, the SI solver (2.19) is equivalent to (2.2) for solving the steady linear equation, therefore we only need to consider (2.2) below.

2.4 The radiative transfer equation and its DG discretization in two spatial dimension

We first consider a steady-state, one-group, isotropically scattering transfer equation

$$\boldsymbol{\Omega}\cdot\nabla_{\boldsymbol{r}} I(\boldsymbol{r},\boldsymbol{\Omega}) + \sigma_t I(\boldsymbol{r},\boldsymbol{\Omega}) = \frac{\sigma_s}{4\pi}\int_S I(\boldsymbol{r},\boldsymbol{\Omega})d\boldsymbol{\Omega} + q(\boldsymbol{r},\boldsymbol{\Omega}), \tag{2.20}$$

where $I(\boldsymbol{r},\boldsymbol{\Omega})$ is the radiative intensity in the direction $\boldsymbol{\Omega}$ and the spatial position $\boldsymbol{r}$, S is the unit sphere, $\sigma_s \geq 0$ is the scattering coefficient of the medium, σ_t is the extinction coefficient of the medium due to both absorption and scattering (namely $\sigma_t \geq \sigma_s$), and $q(\boldsymbol{r},\boldsymbol{\Omega})$ is a given source term. For two spatial dimensional problems, the position vector $\boldsymbol{r}=(x,y)\in\mathcal{D}\subset\mathbb{R}^2$ and the vector is usually described by a polar angle ϕ measured with respect to a fixed axis in space and a corresponding azimuthal angle ψ. If we introduce $\mu=\cos\phi$, we would like to denote

$$d\boldsymbol{r} = dxdy, \quad d\boldsymbol{\Omega} = \sin\phi d\phi d\psi = -d\mu d\psi.$$

To solve the above radiative transfer equation numerically, we need to make use of the DOM and DG method to discretize the angular variables and the spatial variables in (2.20) respectively. For each discrete direction $\boldsymbol{\Omega}_{m,l}=(\zeta_m,\lambda_l), m=1,\ldots,M, l=1,\ldots,L$, with the numbers M,L of directions in ζ and λ respectively, where $\zeta=\sin\phi\cos\psi=\sqrt{1-\mu^2}\cos\psi$ and $\lambda=\sin\phi\sin\psi=\sqrt{1-\mu^2}\sin\psi$, the equation (2.20) turns into a spatial differential equation defined in Cartesian coordinates

$$\zeta_m\frac{\partial I_{m,l}(x,y)}{\partial x} + \lambda_l\frac{\partial I_{m,l}(x,y)}{\partial y} + \sigma_t I_{m,l}(x,y) = \frac{\sigma_s}{4\pi}\sum_{m',l'}\omega_{m',l'}I_{m',l'}(x,y) + q_{m,l}(x,y), \tag{2.21}$$

where $I_{m,l}(x,y) = I(x,y,\zeta_m,\lambda_l)$ is the radiative intensity in the direction (ζ_m,λ_l), $q_{m,l}(x,y) = q(x,y,\zeta_m,\lambda_l)$ is the source term and $\omega_{m,l}$ is the quadrature weight with $\sum_{m',l'} \omega_{m',l'} = 4\pi$.

Here we take the case of $\zeta_m > 0, \lambda_l > 0$ as an example, the DOM-DG scheme for solving (2.20) in a rectangular cell $S_{i,j}$ can be described as

$$\begin{aligned}
&-\int_{S_{i,j}} I_{m,l}(x,y)(\zeta_m v_x(x,y) + \lambda_l v_y(x,y))dxdy + \zeta_m \int_{y_{j-\frac{1}{2}}}^{y_{j+\frac{1}{2}}} I_{m,l}(x^-_{i+\frac{1}{2}},y)v(x^-_{i+\frac{1}{2}},y)dy \\
&+ \lambda_l \int_{x_{i-\frac{1}{2}}}^{x_{i+\frac{1}{2}}} I_{m,l}(x,y^-_{j+\frac{1}{2}})v(x,y^-_{j+\frac{1}{2}})dx + \sigma_t \int_{S_{i,j}} I_{m,l}(x,y)v(x,y)dxdy \\
=\ & \frac{\sigma_s}{4\pi}\int_{S_{i,j}} \varphi(x,y)v(x,y)dxdy + \int_{S_{i,j}} q_{m,l}(x,y)v(x,y)dxdy \\
&+ \zeta_m \int_{y_{j-\frac{1}{2}}}^{y_{j+\frac{1}{2}}} I_{m,l}(x^-_{i-\frac{1}{2}},y)v(x^+_{i-\frac{1}{2}},y)dy + \lambda_l \int_{x_{i-\frac{1}{2}}}^{x_{i+\frac{1}{2}}} I_{m,l}(x,y^-_{j-\frac{1}{2}})v(x,y^+_{j-\frac{1}{2}})dx
\end{aligned} \tag{2.22}$$

with

$$\varphi(x,y) = \sum_{m',l'} \omega_{m',l'} I_{m',l'}(x,y).$$

The scheme for the other cases of (ζ_m,λ_l) is similar, where the numerical flux at the cell interfaces is chosen to be the upwind flux.

Similarly, for the two-dimensional unsteady radiative transfer equation which reads as

$$\frac{1}{c}\frac{\partial I(\boldsymbol{r},\boldsymbol{\Omega},t)}{\partial t} + \boldsymbol{\Omega}\cdot\nabla_{\boldsymbol{r}} I(\boldsymbol{r},\boldsymbol{\Omega},t) + \sigma_t I(\boldsymbol{r},\boldsymbol{\Omega},t) = \frac{\sigma_s}{4\pi}\int_S I(\boldsymbol{r},\boldsymbol{\Omega},t)d\boldsymbol{\Omega} + q(\boldsymbol{r},\boldsymbol{\Omega},t), \tag{2.23}$$

the corresponding DOM-DG scheme for the direction $\zeta_m > 0, \lambda_l > 0$ with backward Euler time discretization has the following form

$$\begin{aligned}
&-\int_{S_{i,j}} I^{n+1}_{m,l}(x,y)(\zeta_m v_x(x,y) + \lambda_l v_y(x,y))dxdy + \zeta_m \int_{y_{j-\frac{1}{2}}}^{y_{j+\frac{1}{2}}} I^{n+1}_{m,l}(x^-_{i+\frac{1}{2}},y)v(x^-_{i+\frac{1}{2}},y)dy \\
&+ \lambda_l \int_{x_{i-\frac{1}{2}}}^{x_{i+\frac{1}{2}}} I^{n+1}_{m,l}(x,y^-_{j+\frac{1}{2}})v(x,y^-_{j+\frac{1}{2}})dx + \widetilde{\sigma}_t \int_{S_{i,j}} I^{n+1}_{m,l}(x,y)v(x,y)dxdy \\
=\ & \frac{\sigma_s}{4\pi}\int_{S_{i,j}} \varphi^{n+1}(x,y)v(x,y)dxdy + \int_{S_{i,j}} \widetilde{q}_{m,l}(x,y)v(x,y)dxdy \\
&+ \zeta_m \int_{y_{j-\frac{1}{2}}}^{y_{j+\frac{1}{2}}} I^{n+1}_{m,l}(x^-_{i-\frac{1}{2}},y)v(x^+_{i-\frac{1}{2}},y)dy + \lambda_l \int_{x_{i-\frac{1}{2}}}^{x_{i+\frac{1}{2}}} I^{n+1}_{m,l}(x,y^-_{j-\frac{1}{2}})v(x,y^+_{j-\frac{1}{2}})dx,
\end{aligned} \tag{2.24}$$

where $\widetilde{\sigma}_t = \sigma_t + \frac{1}{c\Delta t^n}$ and $\widetilde{q}_{m,l}(x,y) = q_{m,l}^{n+1}(x,y) + \frac{1}{c\Delta t^n} I_{m,l}^n(x,y)$. This is the same as (2.22) in the steady case.

For both the steady and unsteady problems, we will utilize the SI method, which allows us to rewrite the DG scheme (2.22) into

$$\begin{aligned}
&-\int_{S_{i,j}} I_{m,l}^{(\ell+1)}(x,y)(\zeta_m v_x(x,y) + \lambda_l v_y(x,y))dxdy + \zeta_m \int_{y_{j-\frac{1}{2}}}^{y_{j+\frac{1}{2}}} I_{m,l}^{(\ell+1)}(x_{i+\frac{1}{2}}^-, y)v(x_{i+\frac{1}{2}}^-, y)dy \\
&+ \lambda_l \int_{x_{i-\frac{1}{2}}}^{x_{i+\frac{1}{2}}} I_{m,l}^{(\ell+1)}(x, y_{j+\frac{1}{2}}^-)v(x, y_{j+\frac{1}{2}}^-)dx + \sigma_t \int_{S_{i,j}} I_{m,l}^{(\ell+1)}(x,y)v(x,y)dxdy \\
= \;& \frac{\sigma_s}{4\pi} \int_{S_{i,j}} \varphi^{(*)}(x,y)v(x,y)dxdy + \int_{S_{i,j}} q_{m,l}(x,y)v(x,y)dxdy \\
&+ \zeta_m \int_{y_{j-\frac{1}{2}}}^{y_{j+\frac{1}{2}}} I_{m,l}^{(\ell+1)}(x_{i-\frac{1}{2}}^-, y)v(x_{i-\frac{1}{2}}^+, y)dy + \lambda_l \int_{x_{i-\frac{1}{2}}}^{x_{i+\frac{1}{2}}} I_{m,l}^{(\ell+1)}(x, y_{j-\frac{1}{2}}^-)v(x, y_{j-\frac{1}{2}}^+)dx,
\end{aligned} \tag{2.25}$$

where

$$\varphi^{(*)}(x,y) = \sum_{m',l'} \omega_{m',l'} I_{m',l'}^{(*)}(x,y).$$

Similarly to the one-dimensional case, $I_{m',l'}^{(*)}(x,y)$ is taken as $I_{m',l'}^{(\ell+1)}(x,y)$ if it has been already obtained; otherwise, it is taken as $I_{m',l'}^{(\ell)}(x,y)$. Notice again that the SI solver (2.25) is equivalent to (2.8) for solving the steady linear equation, therefore we only need to consider (2.8) below.

3 High order positivity-preserving DG schemes for the linear hyperbolic equation and the radiative transfer equation in one spatial dimension

A DG scheme for the linear hyperbolic equations and the radiative transfer equations mentioned in the previous section is called positivity-preserving if it can always generate a non-negative numerical solution when a non-negative source term and non-negative boundary conditions (for time-dependent problems, also a non-negative initial condition) are given.

Generally speaking, high order approximations can provide more accurate solutions but may also produce negative numerical solutions even though the exact solution is positive,

which is un-physical and may sometimes lead to instability of the numerical schemes. In this section we will discuss how to design a high order conservative (in the sense that the cell averages produced by the unmodulated DG solver are not altered) positivity-preserving DG scheme in one spatial dimension. The discussion is restricted to the DG scheme (2.2) solving linear steady-state hyperbolic equations only, however by our discussion in the previous section, it applies also to the DG scheme (2.6) for solving the unsteady linear equation with backward Euler time stepping, and to the DG scheme (2.19) for solving the SI DG solver for steady or unsteady radiative transfer equations.

In each interval S_i, we define

$$\delta_k(x) = \frac{1}{\Delta x_i} \sum_{n=0}^{k} (2n+1) p_n(\xi(x)), \quad x \in S_i \tag{3.1}$$

where $p_n(\xi)$ is the standard Legendre polynomial defined in $[-1, 1]$ and $\xi = \frac{2(x-x_i)}{\Delta x_i}$ with the midpoint of the cell $x_i = \frac{1}{2}(x_{i-\frac{1}{2}} + x_{i+\frac{1}{2}})$. Then the following lemma (see, e.g. [10]) indicates that this polynomial actually defines the δ-function in $P^k(S_i)$ at the point $x_{i+\frac{1}{2}}$. This is also sometimes referred to as the lifting operator in the DG literature.

Lemma 3.1. [10] *For the function $\delta_k(x)$ defined in* (3.1) *and any polynomial $u(x) \in P^k(S_i)$, there always holds*

$$u(x^-_{i+\frac{1}{2}}) = \int_{S_i} u(x)\delta_k(x)dx. \tag{3.2}$$

The proof of this lemma is straightforward, see, e.g. [10].

By Lemma 3.1, we are able to rewrite the left-hand side of (2.2) as

$$LHS = \int_{S_i} u(x) \left(\gamma v(x) - \alpha v'(x) + \alpha v^-_{i+\frac{1}{2}} \delta_k(x) \right) dx. \tag{3.3}$$

We would like to find a special test function $v(x) \in V_h^k$ such that the left-hand side of (2.2) provides the cell average of $u(x)$ multiplied by the cell size, i.e.

$$LHS = \int_{S_i} u(x) \left(\gamma v(x) - \alpha v'(x) + \alpha v^-_{i+\frac{1}{2}} \delta_k(x) \right) dx = \int_{S_i} u(x)dx = \Delta x_i \cdot \overline{u}_i, \quad \forall u(x) \in V_h^k. \tag{3.4}$$

That is, we would like to find $v(x) \in V_h^k$ such that

$$\gamma v(x) - \alpha v'(x) + \alpha v^-_{i+\frac{1}{2}} \delta_k(x) = 1. \tag{3.5}$$

The existence and uniqueness of such a specific test function $v(x)$ are not difficult to prove. More importantly, the fact that $v(x)$ is a polynomial enables us to determine $v(x)$ explicitly as follows

$$v(x) = \begin{cases} \dfrac{1}{\gamma} \cdot \dfrac{1 + \sum\limits_{l=0}^{k} (\frac{\alpha}{\gamma})^{l+1} \left(\delta_k^{(l)}(x_{i+\frac{1}{2}}) - \delta_k^{(l)}(x) \right)}{1 + \sum\limits_{l=0}^{k} (\frac{\alpha}{\gamma})^{l+1} \delta_k^{(l)}(x_{i+\frac{1}{2}})}, & \text{if } \gamma > 0, \\ \dfrac{1}{\alpha}(x_{i+\frac{1}{2}} - x), & \text{if } \gamma = 0. \end{cases} \tag{3.6}$$

Lemma 3.2. *The test function $v(x)$ defined in (3.6) satisfies*

$$v(x) \geq 0, \quad \forall x \in S_i.$$

Proof. For the case of $\gamma = 0$, the result is obvious. Now we consider the case of $\gamma > 0$. To prove it, let us recall a few properties of the standard Legendre polynomials:

$$p_0(\xi) = 1, \quad p_1(\xi) = \xi,$$

and

$$(2n+1)p_n(\xi) = p'_{n+1}(\xi) - p'_{n-1}(\xi), \quad \forall n \geq 2, \quad \xi \in [-1, 1]$$

the latter relation tells us that for all $n \geq 2$,

$$p'_n(\xi) = \begin{cases} \sum\limits_{\substack{k=1 \\ k \text{ is even}}}^{n-1} (2k+1)p_k(\xi) + 1, & \text{if } n \text{ is odd} \\ \sum\limits_{\substack{k=1 \\ k \text{ is odd}}}^{n-1} (2k+1)p_k(\xi), & \text{if } n \text{ is even} \end{cases}$$

By induction, we can express $p_n^{(l)}(\xi), n = 0, 1, \cdots, k, l = 0, 1, \cdots, n$ as a linear combination of Legendre polynomials themselves with positive coefficients. Thanks to $p_n(1) = 1$ for all n and the fact that the maximum value of Legendre polynomials always occurs at the point $\xi = 1$, we know $p_n^{(l)}(1) > 0$ and

$$p_n^{(l)}(1) - p_n^{(l)}(\xi) \geq 0, \quad \forall \xi \in [-1, 1],$$

which implies

$$\delta_k^{(l)}(x_{i+\frac{1}{2}}) > 0, \quad \delta_k^{(l)}(x_{i+\frac{1}{2}}) - \delta_k^{(l)}(x) \geq 0.$$

This clearly leads to the positivity of $v(x)$. □

From the Lemmas above, we know that there exists a unique positive test function $v(x)$ such that the left-hand side of (2.2) is the integral of $u(x)$ over the cell for any $u(x) \in P^k(S_i)$. At the same time, the positivity of $v(x)$ and the source term $f(x)$ guarantee that the right-hand side of (2.2) is also positive for any given positive inflow condition. We have therefore proved the following important conclusion for the unmodulated DG solver (2.2).

Theorem 3.3. *For the linear steady-state hyperbolic equation in* (2.1)*, if the inflow boundary condition from the upstream cell (including the physical boundary condition for the first cell) and the source term are both positive, then the cell average* $\overline{u}_i$ *of the unmodulated DG scheme is positive.*

If the unmodulated DG solver (2.2) is used, there is still one condition required to prove that all the cell averages of the unmodulated DG solution are positive, namely all the upstream DG solution values at the interfaces $u^-_{i+\frac{1}{2}}$ remain positive, when the physical inflow condition and the source term are both positive. This is actually correct, when the mesh size h is small enough, as proved in Appendix B. However, the result in Appendix B is not required for the following development of the conservative positivity-preserving DG schemes.

3.1 Positivity-preserving limiter

The crucial Theorem 3.3 enables us to achieve the positivity of the numerical solution $u(x)$ in the cell S_i by utilizing the scaling positivity-preserving limiter proposed in [15], without losing the designed high order accuracy. Before describing the limiting procedure, let us first introduce the Gauss-Lobatto point set in the cell S_i as G_i

$$G_i = \left\{ x_{i-\frac{1}{2}} = x_i^1, x_i^2, \cdots, x_i^K = x_{i+\frac{1}{2}} \right\},$$

where K is chosen so that integrals for P^k polynomials are given exactly by the Gauss-Lobatto quadrature. Then the specific implementation of the limiter can be taken as follows:

$$\widetilde{u}_i(x) = \theta(u_i(x) - \overline{u}_i) + \overline{u}_i \tag{3.7}$$

with

$$\theta = \min_{x \in G_i} \left\{ 1, \left| \frac{\overline{u}_i}{\overline{u}_i - u_i(x)} \right| \right\}. \tag{3.8}$$

By this limitation, we can get the approximating polynomial $\widetilde{u}_i(x)$ which is positive at all Gauss-Lobatto points (including at the right boundary of the cell, thus making Theorem 3.3 valid for the neighboring cell downstream), without loss of accuracy.

We have therefore obtained a high order DG scheme, which is the original DG scheme (2.2) plus the scaling limiter (3.7)-(3.8), that achieves positivity for the numerical solution at all Gauss-Lobatto points in each cell, as well as being conservative in the sense that the cell averages from the unmodulated DG solver is not changed by the limiter (3.7)-(3.8). This conclusion is valid for DG schemes solving both steady and unsteady linear hyperbolic equations and for the SI DG solver of steady and unsteady radiative transfer equations.

4 High order positivity-preserving DG schemes for the linear hyperbolic equation and the radiative transfer equation in two spatial dimensions

We would like to repeat our work in one-dimension and find a specific test function $v(x, y) \in V_h^k$ such that, for any $u(x, y) \in V_h^k$, the left-hand side of (2.8) produces the integral of $u(x, y)$ over the cell $S_{i,j}$:

$$LHS = \int_{S_{i,j}} u(x, y) dx dy. \tag{4.1}$$

Similarly as in the one-dimensional case, we can still easily obtain the existence and uniqueness of such test function $v(x, y)$. If we could also establish the fact that $v(x, y)$ is positive in the cell $S_{i,j}$, then the same result as in one-dimension would hold. Unfortunately, it appears that this particular $v(x, y)$ is negative in part of the cell $S_{i,j}$ for both the P^k (polynomials

of degree at most k) and the Q^k (tensor-product polynomials of degree k) DG spaces. We would then attempt to modify the DG space, by augmenting P^k with additional functions (P^k is retained in the space to ensure accuracy), so that the test function $v(x, y)$ determined by (4.1) in this augmented space is positive in $S_{i,j}$. We will denote this augmented space as R^k. In this paper we only attempt to carry this procedure out for $k = 1$ (the second order DG method) on rectangular meshes, as an example.

4.1 The positivity-preserving DG scheme with $k = 1$

Before starting the procedure of finding positivity-preserving DG scheme with an augmented DG space R^1, let us first show that the specific test function $v(x, y)$ satisfying (4.1) does not remain positive for either the P^1 or the Q^1 space.

As before, let $S_{i,j}$ be the rectangular element with center (x_i, y_j) and width $\Delta x_i, \Delta y_j$. For simplicity we take $\Delta x_i = \Delta y_j$, as a change in this mesh ratio only alters the parameters α and β in (2.8). If we denote

$$\xi = \frac{2(x - x_i)}{\Delta x_i}, \quad \eta = \frac{2(y - y_j)}{\Delta y_j}, \tag{4.2}$$

then we can obtain the specific test function $v(x, y)$ satisfying (4.1) by solving a local linear system. For P^1, we obtain

$$\begin{aligned} v(\xi,\eta) =& \frac{\Delta x_i}{\Lambda_1}\big((\beta+\gamma\Delta x_i)(\gamma\Delta x_i+3\beta(1-\eta)) \\ &+\alpha(\beta(10-9\xi-9\eta)+\gamma\Delta x_i(4-3\xi))+3\alpha^2(1-\xi)\big) \end{aligned} \tag{4.3}$$

where

$$\Lambda_1 = 6\alpha^3+6\beta^3+10\beta^2\gamma\Delta x_i+5\beta\gamma^2\Delta x_i^2+\gamma^3\Delta x_i^3+2\alpha^2(11\beta+5\gamma\Delta x_i)+\alpha(22\beta^2+18\beta\gamma\Delta x_i+5\gamma^2\Delta x_i^2).$$

Similarly, for Q^1, we obtain

$$\begin{aligned} v(\xi,\eta) =& \frac{\Delta x_i}{\Lambda_2}\big((6\beta^2+4\beta\gamma\Delta x_i+\gamma^2\Delta x_i^2)(\gamma\Delta x_i+3\beta(1-\eta)) \\ &+\alpha(2\beta\gamma\Delta x_i(17-9\xi-9\eta+9\xi\eta)+\gamma^2\Delta x_i^2(7-3\xi)+6\beta^2(7-3\xi-6\eta+6\xi\eta)) \\ &+18\alpha^3(1-\xi)+6\alpha^2(\gamma\Delta x_i(3-2\xi)+\beta(7-6\xi-3\eta+6\xi\eta))\big) \end{aligned} \tag{4.4}$$

where

$$\Lambda_2 = 36\alpha^4 + 48\alpha^3(2\beta + \gamma\Delta x_i) + (6\beta^2 + 4\beta\gamma\Delta x_i + \gamma^2\Delta x_i^2)^2$$
$$+ 4\alpha^2(30\beta^2 + 28\beta\gamma\Delta x_i + 7\gamma^2\Delta x_i^2) + 8\alpha(12\beta^3 + 14\beta^2\gamma\Delta x_i + 6\beta\gamma^2\Delta x_i^2 + \gamma^3\Delta x_i^3).$$

We plot these two test functions in Figures 4.1-4.2. Clearly, we see that they are negative in certain parts of the cell $S_{i,j}$.

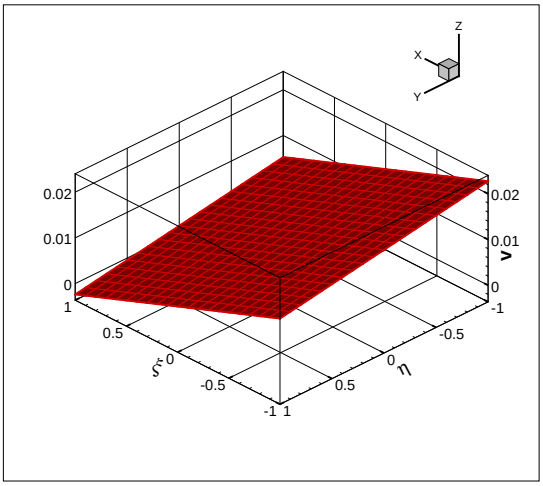

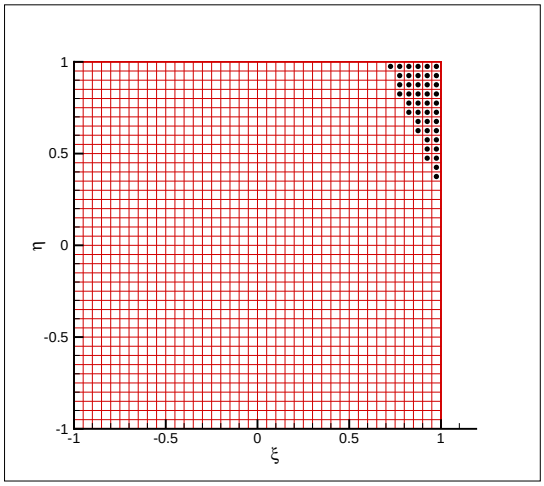

Figure 4.1: The test function $v(\xi, \eta)$ in P^1 with $\alpha = 4, \beta = 1, \gamma = 10, \Delta x_i = \Delta y_j = 0.1$. Left: the surface plot of v; Right: the region plot of v. The black points in the figure represent the area where v is negative.

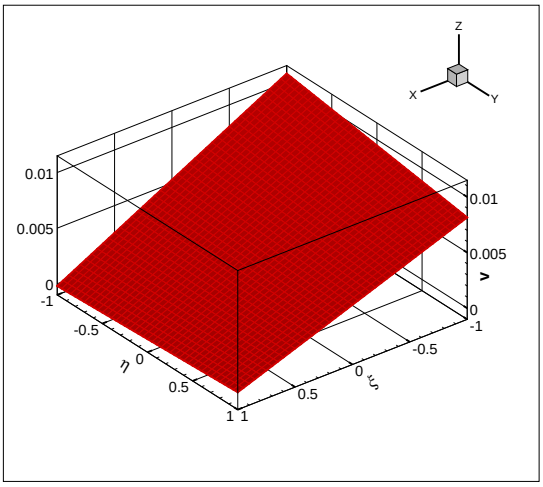

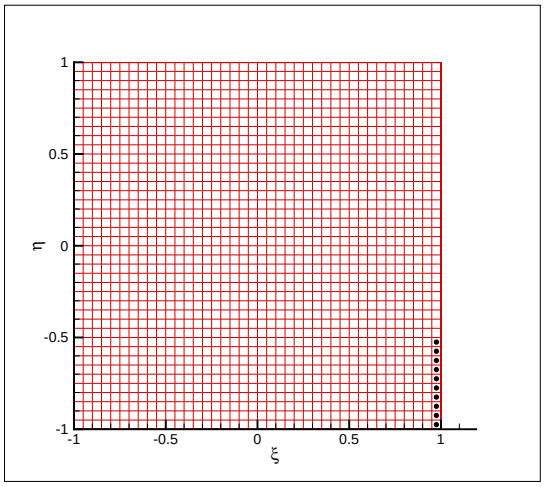

Figure 4.2: The test function $v(\xi, \eta)$ in Q^1 with $\alpha = 10, \beta = 1, \gamma = 0, \Delta x_i = \Delta y_j = 0.1$. Left: the surface plot of v; Right: the region plot of v. The black points in the figure represent the area where v is negative.

We now attempt to construct an augmented DG space R^k, such that the specific test

function $v(x,y)$ determined by (4.1) remains positive over the cell $S_{i,j}$. We start with augmenting P^1 by adding just one function, such that the computational cost is the same as that for Q^1. If we choose standard Legendre polynomials as the basis functions of P^1 denoted as $\{1,\xi,\eta\}$, then our ansatz for this additional function is $\xi\eta+\mu(\xi^2+\eta^2)$ where μ is a parameter to be determined. Then the augmented DG space R^1 is

$$R^1 = Span\left\{1,\xi,\eta,\xi\eta+\mu(\xi^2+\eta^2)\right\}. \tag{4.5}$$

It turns out that the choice of $\mu=\frac{1}{4}$ would produce a $v(x,y)$ satisfying (4.1) which is positive over $S_{i,j}$, the details of this $v(x,y)$ is given in Appendix A. We would like to remark that neither the choice of the additional function $\xi\eta+\mu(\xi^2+\eta^2)$ nor the choice of the parameter $\mu=\frac{1}{4}$ is unique.

Since we know that there exists a positive $v(x,y)$ satisfying (4.1), we can get the following important conclusion.

Theorem 4.1. *Consider the linear steady-state hyperbolic equation in* (2.7)*, then the cell average* $\overline{u}_{i,j}$ *of the DG scheme* (2.8) *with the augmented DG space* R^1 *defined in* (4.5) *will remain positive if positive inflow conditions from the upstream cells (including the physical boundary conditions for the boundary cells) and positive source terms are given.*

Theorem 4.1 motivates us to obtain the positivity of the numerical approximation $u(x,y)$ in the cell $S_{i,j}$ as before by applying the scaling positivity-preserving limiter without the loss of the designed accuracy. Now, let us first denote the Gauss-Lobatto point set in the cell $S_{i,j}$ as $G_{i,j}$, which consists of the vertices of the cells, the midpoints of each edge of the cells as well as the center point of the cell, namely

$$G_{i,j} = \left\{(x_i^{K_1}, y_j^{K_2}) : K_1, K_2 = 1,2,3\right\}$$

with $x_i^1 = x_{i-\frac{1}{2}}, x_i^2 = x_i, x_i^3 = x_{i+\frac{1}{2}}$, so does $y_j^{K_2}$. Then the limiting procedure can be described as the following modification of the approximate polynomial

$$\widetilde{u}_{i,j}(x,y) = \theta(u_{i,j}(x,y)-\overline{u}_{i,j})+\overline{u}_{i,j} \tag{4.6}$$

where

$$\theta = \min_{(x,y)\in G_{i,j}} \left\{ 1, \left| \frac{\overline{u}_{i,j}}{\overline{u}_{i,j} - u_{i,j}(x,y)} \right| \right\}. \tag{4.7}$$

5 Numerical tests

In this section, we perform numerical experiments in one- and two-dimensions to validate the properties of high order accuracy and positivity-preserving of our DG schemes. We adopt S_8 and P_8-T_8 discrete-ordinate quadrature rules for all the following one-dimensional and the two-dimensional tests with non-zero scattering terms respectively, unless otherwise stated.

Example 1. (Accuracy test of the DG scheme for the one-dimensional steady advection equation)

We solve the steady advection equation (2.1) with $\alpha = 1$, $\gamma = 6000$ and $f(x) = \gamma(\frac{1}{9}\cos^4 x + \varepsilon) - \frac{4}{9}\cos^3 x \sin x$. Here we take $\varepsilon = 10^{-14}$ to ensure the source term to be nonnegative. The computational domain is $[0, \pi]$. The boundary condition is given as $u(0) = \frac{1}{9} + \varepsilon$. The exact solution for this problem is $u(x) = \frac{1}{9}\cos^4 x + \varepsilon$. We record the numerical errors, orders of accuracy, and the minimum values of the numerical approximation polynomials. The results with and without the positivity-preserving limiter are given in Tables 5.1-5.2. We can see that the minimum value of the numerical solutions is negative for the unmodulated DG scheme. Also, the designed high order accuracy is maintained with the application of the positivity-preserving limiter, verifying our theoretical results.

Table 5.1: Errors of the P^k DG scheme for solving the steady problem (2.1) using N uniform cells without the positivity-preserving limiter

k	N	L_2 error	L_2 order	L_∞ error	L_∞ order	$\min u_h$
1	10	0.14E-02	–	0.33E-02	–	-0.48E-03
	20	0.36E-03	1.98	0.89E-03	1.89	-0.58E-04
	40	0.94E-04	1.99	0.22E-03	1.96	-0.41E-05
	80	0.22E-04	1.99	0.58E-04	1.96	-0.27E-06
	160	0.56E-05	1.99	0.14E-04	1.96	-0.17E-07
	320	0.14E-05	1.99	0.39E-05	1.93	-0.11E-08
2	10	0.11E-03	–	0.30E-03	–	-0.35E-04
	20	0.15E-04	2.98	0.38E-04	2.99	-0.24E-05
	40	0.18E-05	2.99	0.48E-05	2.99	-0.16E-06
	80	0.23E-06	2.99	0.59E-06	3.01	-0.10E-07
	160	0.29E-07	2.99	0.73E-07	3.02	-0.66E-09
	320	0.37E-08	2.98	0.88E-08	3.04	-0.45E-10
3	10	0.87E-05	–	0.22E-04	–	-0.12E-04
	20	0.55E-06	3.98	0.15E-05	3.82	-0.93E-06
	40	0.34E-07	3.99	0.10E-06	3.91	-0.62E-07
	80	0.21E-08	3.99	0.67E-08	3.93	-0.41E-08
	160	0.13E-09	3.99	0.44E-09	3.91	-0.27E-09
	320	0.87E-11	3.97	0.30E-10	3.87	-0.18E-10
4	10	0.54E-06	–	0.15E-05	–	-0.73E-06
	20	0.17E-07	4.98	0.47E-07	4.96	-0.12E-07
	40	0.53E-09	4.99	0.14E-08	5.03	-0.20E-09
	80	0.16E-10	4.99	0.44E-10	5.04	-0.33E-11
	160	0.52E-12	4.98	0.13E-11	5.07	-0.46E-13
	320	0.16E-13	4.96	0.39E-13	5.05	0.90E-14

Table 5.2: Errors of the P^k DG scheme for solving the steady problem (2.1) using N uniform cells with the positivity-preserving limiter

k	N	L_2 error	L_2 order	L_∞ error	L_∞ order	Limited cells (%)
1	10	0.14E-02	–	0.33E-02	–	40.00
	20	0.36E-03	2.00	0.89E-03	1.89	20.00
	40	0.90E-04	1.99	0.23E-03	1.96	10.00
	80	0.22E-04	1.99	0.58E-04	1.96	5.00
	160	0.56E-05	1.99	0.15E-04	1.96	2.50
	320	0.14E-05	1.99	0.39E-05	1.93	1.25
2	10	0.12E-03	–	0.30E-03	–	20.00
	20	0.15E-04	3.02	0.38E-04	2.99	10.00
	40	0.19E-05	3.00	0.48E-05	2.99	5.00
	80	0.24E-06	2.99	0.60E-06	3.01	2.50
	160	0.29E-07	2.99	0.73E-07	3.02	1.25
	320	0.37E-08	2.98	0.88E-08	3.04	0.63
3	10	0.15E-04	–	0.55E-04	–	20.00
	20	0.84E-06	4.14	0.42E-05	3.70	10.00
	40	0.45E-07	4.21	0.28E-06	3.93	5.00
	80	0.25E-08	4.16	0.17E-07	3.98	2.50
	160	0.15E-09	4.09	0.11E-08	3.99	1.25
	320	0.90E-11	4.03	0.69E-10	3.99	0.63
4	10	0.92E-06	–	0.22E-05	–	20.00
	20	0.19E-07	5.58	0.48E-07	5.52	10.00
	40	0.54E-09	5.14	0.14E-08	5.03	5.00
	80	0.17E-10	5.01	0.44E-10	5.04	2.50
	160	0.53E-12	4.98	0.13E-11	5.07	1.25
	320	0.17E-13	4.96	0.39E-13	5.05	0.00

Example 2. (Accuracy test of the DG scheme for the one-dimensional linear time-dependent hyperbolic equation)

We solve the time-dependent problem (2.3) with $\alpha = 1$, $\gamma = 1$ and $f(x,t) = \cos^4(x-t)+\varepsilon$ with the final time $T = 0.1$. Here we also take $\varepsilon = 10^{-14}$. The computational domain is $[0, \pi]$. The initial condition and boundary condition are given as $u(x,0) = \cos^4(x) + \varepsilon$ and $u(0,t) = \cos^4(t)+\varepsilon$ respectively. The exact solution for this problem is $u(x,t) = \cos^4(x-t)+\varepsilon$. The time step is taken as $\Delta t = \text{CFL} \cdot h^{k+1}$ (with CFL = 10 for $k \geq 2$ and CFL = 1 for $k = 1$) to ensure that the temporal error does not dominate. We record the numerical errors and orders of accuracy by performing the DG scheme without and with the positivity-preserving

limiter, respectively. The results are shown in Tables 5.3-5.4. We also list the minimum value of the numerical approximation polynomials after one time step in Table 5.3, and the percentage of cells where the limiter is used in Table 5.4. We can see that the limiter indeed works and does not destroy the high order accuracy.

Table 5.3: Errors of the P^k DG scheme for solving the time-dependent problem (2.3) using N uniform cells without the positivity-preserving limiter

k	N	L_2 error	L_2 order	L_∞ error	L_∞ order	$\min u_h$
	20	0.64E-02	–	0.13E-01	–	-0.89E-03
	40	0.16E-02	1.95	0.39E-02	1.72	-0.53E-04
1	80	0.41E-03	1.99	0.99E-03	1.98	-0.30E-05
	160	0.10E-03	2.00	0.24E-03	2.01	-0.17E-06
	320	0.26E-04	2.00	0.61E-04	2.00	-0.10E-07
	20	0.53E-02	–	0.62E-02	–	0.27E-05
	40	0.77E-03	2.80	0.90E-03	2.77	-0.17E-05
2	80	0.97E-04	2.97	0.11E-03	2.96	-0.10E-06
	160	0.12E-04	2.99	0.14E-04	2.99	-0.56E-08
	320	0.15E-05	2.98	0.18E-05	3.00	-0.34E-09
	20	0.96E-03	–	0.11E-02	–	-0.11E-04
	40	0.61E-04	3.96	0.73E-04	3.97	-0.58E-06
3	80	0.38E-05	3.99	0.46E-05	3.97	-0.34E-07
	160	0.24E-06	4.00	0.28E-06	4.01	-0.21E-08
	320	0.15E-07	3.99	0.18E-07	3.98	-0.13E-09
	10	0.44E-02	–	0.51E-02	–	0.11E-04
	20	0.15E-03	4.85	0.18E-03	4.79	-0.12E-07
4	40	0.48E-05	4.99	0.57E-05	5.00	-0.20E-09
	80	0.15E-06	4.99	0.17E-06	5.00	-0.33E-11
	160	0.44E-08	5.07	0.51E-08	5.12	-0.46E-13

Table 5.4: Errors of the P^k DG scheme for solving the time-dependent problem (2.3) using N uniform cells with the positivity-preserving limiter

k	N	L_2 error	L_2 order	L_∞ error	L_∞ order	Limited cells (%)
	20	0.64E-02	–	0.13E-01	–	14.00
	40	0.17E-02	1.94	0.39E-02	1.72	8.08
1	80	0.42E-03	1.99	0.99E-03	1.98	4.26
	160	0.10E-03	2.00	0.24E-03	2.01	2.20
	320	0.26E-04	2.00	0.61E-04	2.00	1.18
	20	0.54E-02	–	6.201E-3	–	0.00
	40	0.77E-03	2.80	0.91E-03	2.77	0.47
2	80	0.98E-04	2.97	0.11E-03	2.96	0.16
	160	0.12E-04	2.99	0.14E-04	2.99	0.63E-01
	320	0.15E-05	2.99	0.18E-05	3.00	0.28E-01
	20	0.96E-03	–	0.11E-02	–	2.05
	40	0.61E-04	3.96	0.73E-04	3.97	1.04
3	80	0.38E-05	3.99	0.46E-05	3.97	0.38
	160	0.24E-06	4.00	0.29E-06	4.01	0.13
	320	0.15E-07	3.99	0.18E-07	3.98	0.38E-01
	10	0.44E-02	–	0.51E-02	–	0.00
	20	0.15E-03	4.85	0.18E-03	4.79	0.52
4	40	0.48E-05	4.99	0.57E-05	5.00	0.45
	80	0.15E-06	4.99	0.18E-06	5.00	0.79E-01
	160	0.45E-08	5.07	0.51E-08	5.12	0.13E-01

Example 3. (Shock in the linear problem $u_t + u_x = 0$.)

The initial condition is taken as

$$u(x,0) = \begin{cases} 1, & \text{if } x \in [\frac{1}{4}, \frac{3}{4}] \\ \varepsilon, & \text{otherwise} \end{cases}$$

The boundary condition is $u(0,t) = \varepsilon$ and the computational domain is $[0, \frac{3}{2}]$. The small positive constant $\varepsilon = 10^{-14}$ is used to remove the round-off effect. We simulate this problem using our positivity-preserving DG scheme described in (2.6) up to the time $T = 0.2$. Figure 5.1 shows the comparison of numerical approximations obtained from the $\{P^1, P^2, P^3, P^4\}$ DG schemes without and with the positivity-preserving limiter. We can clearly notice that the DG schemes without the positivity-preserving limiter produce negative solutions while the positivity can be maintained by using the limiter.

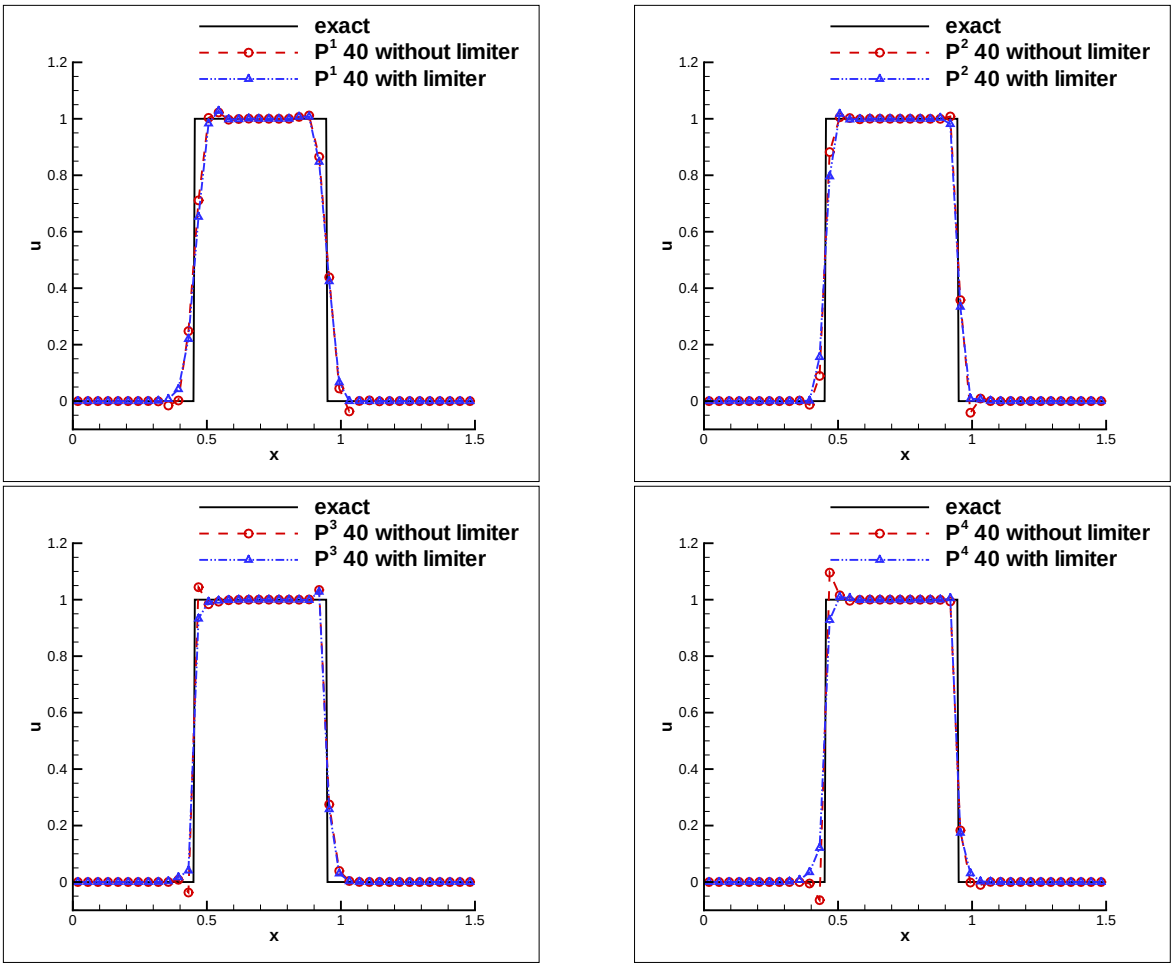

Figure 5.1: The comparison of numerical solutions to the discontinuous problem computed by the $\{P^1, P^2, P^3, P^4\}$ DG schemes without and with positivity-preserving limiter.

Example 4. (Accuracy test of the DG scheme for the one-dimensional steady radiative transfer equation [14])

In this test, we solve the absorbing-scattering radiative transfer problem described by (2.11) with $\sigma_t = 22000, \sigma_s = 1, q(x,\mu) = -4\pi\mu^3 \cos^3 \pi x \sin \pi x + \sigma_t(\mu^2 \cos^4 \pi x + a) - \sigma_s(a + \frac{\cos^4 \pi x}{3})$. Here $a = 10^{-14}$ is a small positive constant which is used to avoid the round-off effect and to ensure the source term to be nonnegative. The computational domain is $[0, 1]$ and the boundary condition is given as follows:

$$\begin{cases} I(0,\mu) = \mu^2 + a \quad \text{if} \quad \mu > 0, \\ I(1,\mu) = \mu^2 + a \quad \text{if} \quad \mu < 0. \end{cases}$$

We have the exact solution for this problem given by $I(x,\mu) = \mu^2 \cos^4 \pi x + a$.

When performing the test on the DG scheme without the positivity-preserving limiter, we record the numerical errors and orders of accuracy as well as the minimum of the numerical approximation polynomials at the Gauss-Lobatto points in Table 5.5. We can see that negative values at the Gauss-Lobatto points do occur. We then apply the positivity-preserving limiter on the DG scheme and show the corresponding numerical errors and orders of accuracy in Table 5.6. The percentage of cells where the positivity-preserving limiter is used is also listed in this table. We can see that the usage of this limiter does not destroy the high order accuracy.

Table 5.5: Errors of the P^k DG scheme for solving the steady radiative transfer equation (2.11) using N uniform cells, without the positivity-preserving limiter

k	N	L_2 error	L_2 order	L_∞ error	L_∞ order	$\min u_h$
1	10	0.29E-02	–	0.27E-01	–	-0.39E-02
	20	0.74E-03	1.98	0.74E-02	1.89	-0.48E-03
	40	0.18E-03	1.99	0.18E-02	1.97	-0.34E-04
	80	0.46E-04	1.99	0.48E-03	1.97	-0.22E-05
	160	0.11E-04	1.99	0.12E-03	1.96	-0.14E-06
	320	0.29E-05	1.99	0.32E-04	1.94	-0.94E-08
2	10	0.25E-03	–	0.25E-02	–	0.19E-04
	20	0.32E-04	2.98	0.32E-03	2.99	0.12E-05
	40	0.41E-05	2.99	0.40E-04	2.99	0.73E-07
	80	0.51E-06	3.00	0.49E-05	3.01	0.46E-08
	160	0.63E-07	3.00	0.61E-06	3.02	0.28E-09
	320	0.79E-08	3.00	0.74E-07	3.04	0.18E-10
3	10	0.20E-04	–	0.18E-03	–	-0.10E-03
	20	0.12E-05	3.98	0.12E-04	3.82	-0.76E-05
	40	0.79E-07	3.99	0.84E-06	3.92	-0.50E-06
	80	0.50E-08	3.99	0.55E-07	3.94	-0.32E-07
	160	0.31E-09	3.99	0.36E-08	3.92	-0.20E-08
	320	0.19E-10	3.98	0.24E-09	3.88	-0.13E-09
4	10	0.13E-05	–	0.12E-04	–	-0.59E-05
	20	0.41E-07	4.98	0.39E-06	4.96	-0.99E-07
	40	0.13E-08	5.00	0.12E-07	5.02	-0.16E-08
	80	0.40E-10	5.01	0.37E-09	5.03	-0.25E-10
	160	0.12E-11	5.02	0.11E-10	5.06	-0.39E-12

Table 5.6: Errors of the P^k DG scheme for solving the steady radiative transfer equation (2.11) using N uniform cells, with the positivity-preserving limiter

k	N	L_2 error	L_2 order	L_∞ error	L_∞ order	Limited cells (%)
1	10	0.29E-02	–	0.27E-01	–	40.00
	20	0.74E-03	2.00	0.74E-02	1.89	20.00
	40	0.18E-03	1.99	0.18E-02	1.97	10.00
	80	0.46E-04	1.99	0.48E-03	1.97	5.00
	160	0.11E-04	1.99	0.12E-03	1.96	2.50
	320	0.29E-05	1.99	0.31E-04	1.94	1.25
2	10	0.25E-03	–	0.25E-02	–	0.00
	20	0.38E-04	2.98	0.32E-03	2.99	0.00
	40	0.41E-05	2.99	0.40E-04	2.99	0.00
	80	0.51E-06	3.00	0.49E-05	3.01	0.00
	160	0.63E-07	3.00	0.62E-06	3.02	0.00
	320	0.79E-08	3.00	0.74E-07	3.04	0.00
3	10	0.32E-04	–	0.45E-03	–	20.00
	20	0.18E-05	4.12	0.35E-04	3.70	10.00
	40	0.10E-06	4.19	0.23E-05	3.93	5.00
	80	0.57E-08	4.14	0.14E-06	3.98	2.50
	160	0.33E-09	4.08	0.91E-08	3.99	1.25
	320	0.20E-10	4.03	0.57E-09	3.99	0.63
4	10	0.19E-05	–	0.18E-04	–	20.00
	20	0.44E-07	5.41	0.39E-06	5.51	10.00
	40	0.13E-08	5.09	0.12E-07	5.02	5.00
	80	0.40E-10	5.02	0.37E-09	5.03	2.50
	160	0.12E-11	5.02	0.11E-10	5.06	1.25

Example 5 (Counter-example in the 2D case)

In this example, we verify that the unmodulated DG solver based on P^1 or Q^1 space can generate negative cell averages in the first cell (i.e. the lower-left corner cell) even though the inflow boundary conditions and the source term are both positive. We consider the following smooth problem:

$$u_x + u_y = \left(\frac{3}{2}(x+y)\right)^{10}, \quad (x,y) \in \left[0,\frac{1}{2}\right] \times \left[0,\frac{1}{2}\right]$$

with the boundary conditions

$$u(x,0) = \frac{\left(\frac{3}{2}\right)^{10} x^{11}}{22}, \quad u(0,y) = \frac{\left(\frac{3}{2}\right)^{10} y^{11}}{22}.$$

Obviously, the analytic solution is formulated as $u(x,y) = \frac{\left(\frac{3}{2}\right)^{10}(x+y)^{11}}{22}$. We simulate the problem numerically using P^1 DG scheme and R^1 DG scheme respectively and obtain the following table of errors and orders. Moreover, we record the cell average values in the first cell (i.e. the lower-left corner cell) for each mesh. It is easy to observe that negative cell averages indeed occur in the first cell with positive boundary conditions and positive source term when using the P^1 DG scheme.

Table 5.7: Errors of the P^1 DG scheme and augmented (R^1) DG scheme for solving the linear hyperbolic equation above using $N_x \times N_y$ uniform cells

	P^1			R^1		
$N_x = N_y$	L_2 error	L_2 order	$\overline{u}_{1,1}$	L_2 error	L_2 order	$\overline{u}_{1,1}$
2	0.83E-01	—	-0.47E-05	0.42E-01	—	0.48E-04
4	0.27E-01	1.59	-0.23E-08	0.96E-02	2.13	0.23E-07
8	0.72E-02	1.93	-0.11E-11	0.22E-02	2.11	0.11E-10
16	0.17E-02	2.01	-0.55E-15	0.56E-03	1.98	0.56E-14
32	0.44E-03	2.01	-0.33E-18	0.14E-03	1.96	0.27E-17

When going to the Q^1 DG scheme, we consider the equation (2.7) locally defined within one cell $[0,\Delta x]\times[0,\Delta y]$ with $\alpha = 5, \gamma = 0$ since it is more difficult to define a global and smooth function which generate negative cell averages. The boundary conditions and source term are given as follows:

$$u(x,0) = u(0,y) = 0, \quad f = \begin{cases} 1001, & \text{if } \frac{487}{496} \le \xi \le 1, -\frac{17}{18} \le \eta \le \frac{60\xi - 67}{24\xi - 15} \\ 0, & \text{otherwise} \end{cases}$$

Then the exact solution reads as

$$u(x,y) = \begin{cases} 200x + y, & \text{if } \frac{487}{496} \le \xi \le 1, -\frac{17}{18} \le \eta \le \frac{60\xi - 67}{24\xi - 15} \\ 0, & \text{otherwise} \end{cases}$$

where ξ and η are defined as (4.2). We compute the cell average by means of the unmodulated DG solver and augmented DG solver respectively with three different meshes by refinement. The numerical approximations are recorded in the Table 5.8. We can see that the Q^1 DG scheme produces negative cell average while R^1 DG scheme does not.

Table 5.8: Comparison of the cell averages $\overline{u}_{1,1}$ computed from Q^1 DG scheme and augmented (R^1) DG scheme

$\Delta x = \Delta y$	exact	Q^1	R^1
1/4	0.12E-02	-0.11E-04	0.12E-03
1/8	0.15E-03	-0.14E-05	0.19E-04
1/16	0.19E-04	-0.17E-06	0.24E-05

Example 6. (The accuracy test of the DG schemes on the purely absorbing model for the two-dimensional steady radiative transfer equation)

In this test, we solve the two-dimensional steady radiative transfer equation (2.21) with $\sigma_t = 1, \sigma_s = 0$, $q = 0$. The computational domain is $[0,1] \times [0,1]$. $\zeta = 0.7, \lambda = 0.3$. The boundary condition is

$$I(x,0) = 0, \qquad I(0,y) = \sin^6(\pi y).$$

In this case, the problem has the exact solution given as follows,

$$I(x,y) = \begin{cases} 0, & y < \frac{\lambda}{\zeta}x, \\ \sin^6(\pi(y - \frac{\lambda}{\zeta}x))e^{-\frac{\sigma_t}{\zeta}x}, & \text{else.} \end{cases}$$

For this problem, numerically negative radiative intensity appears if the positivity-preserving limiter is not used in the high order DG schemes. Figure 5.2 shows the contour of the radiative intensity simulated by the R^1 DG scheme using 40×40 uniform cells and the cells where the positivity-preserving limiter has been performed during the simulation. The errors and orders of accuracy for the R^1 DG scheme without and with the positivity-preserving limiter are listed in Tables 5.9-5.10 respectively. The percentage of the cells that require the usage of the positivity-preserving limiter is listed in the table 5.10 as well. From the table, we can observe the desired order of accuracy for the positivity-preserving R^1 DG scheme, both in L_2-norm and L_∞-norm, which is quite similar to that of the R^1 DG scheme without the positivity-preserving limiter.

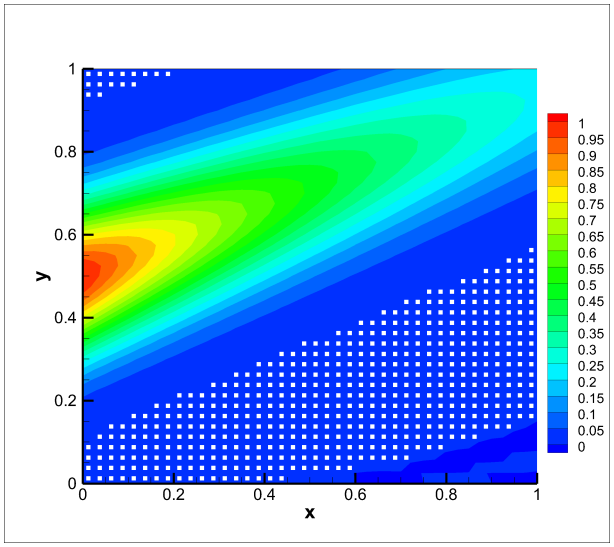

Figure 5.2: The radiative intensity for the purely absorbing model simulated by the R^1 DG scheme with the positivity-preserving limiter on a 40×40 uniform grid. The white points represent the cells where the positivity-preserving limiter has been enacted during the computation.

Table 5.9: Errors of the R^1 DG scheme without positivity-preserving limiter on the purely absorbing model for the 2D steady radiative transfer equation

$N_x = N_y$	L_2 error	L_2 order	L_∞ error	L_∞ order	$\min u_h$
10	0.59E-03	–	0.90E-01	–	-0.28E-01
20	0.15E-03	1.96	0.28E-01	1.70	-0.30E-02
40	0.39E-04	1.99	0.79E-02	1.82	-0.12E-03
80	0.97E-05	1.99	0.21E-02	1.91	-0.42E-05

Table 5.10: Errors of the R^1 DG scheme with positivity-preserving limiter on the purely absorbing model for the 2D steady radiative transfer equation

$N_x = N_y$	L_2 error	L_2 order	L_∞ error	L_∞ order	limited(%)
10	0.62E-03	–	0.90E-01	–	58.00
20	0.16E-03	1.96	0.28E-01	1.69	45.75
40	0.39E-04	2.03	0.79E-02	1.82	31.31
80	0.97E-05	1.99	0.21E-02	1.91	16.97

Example 7. (The positivity-preserving test of the DG schemes on the transparent model for the two-dimensional steady radiative transfer equation)

This problem is a two-dimensional transparent model which is described by the equation

(2.21) with $\sigma_t = 0, \sigma_s = 0, q = 0$. The computational domain is $[0,1]\times[0,1]$. $\zeta = 0.6, \lambda = 0.4$. The boundary condition is $I(x,0) = 0, I(0,y) = 1$. For this problem, it has the exact solution as follows,

$$I(x,y) = \begin{cases} 0, & y < \frac{\lambda}{\zeta}x, \\ 1, & \text{else.} \end{cases}$$

Figure 5.3 plots the contour of the radiative intensity simulated by the R^1 DG scheme with the positivity-preserving limiter on a 40×40 uniform grid. In the figure, we mark the cells where the positivity-preserving has been enacted by discrete white points as well. Figures 5.4 show the comparison of the radiative intensity cut along the lines $y = 0.5$ and $x = 0.5$ simulated by the R^1 DG scheme without and with the positivity-preserving limiter respectively. We can clearly see that the R^1 DG scheme without the positivity-preserving limiter produces negative solutions while the positivity of the radiative intensity can be kept well for the R^1 DG scheme with the positivity-preserving limiter.

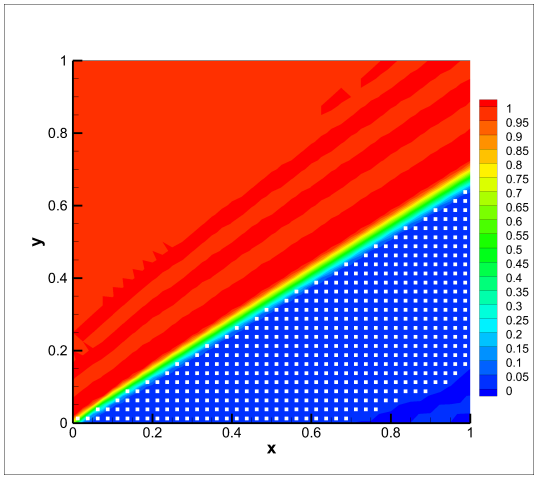

Figure 5.3: The contour of the radiative intensity for the transparent model simulating by the R^1 DG scheme with the positivity-preserving limiter on a 40×40 uniform grid. The white points represent the cells where the positivity-preserving limiter has been enacted during the computation.

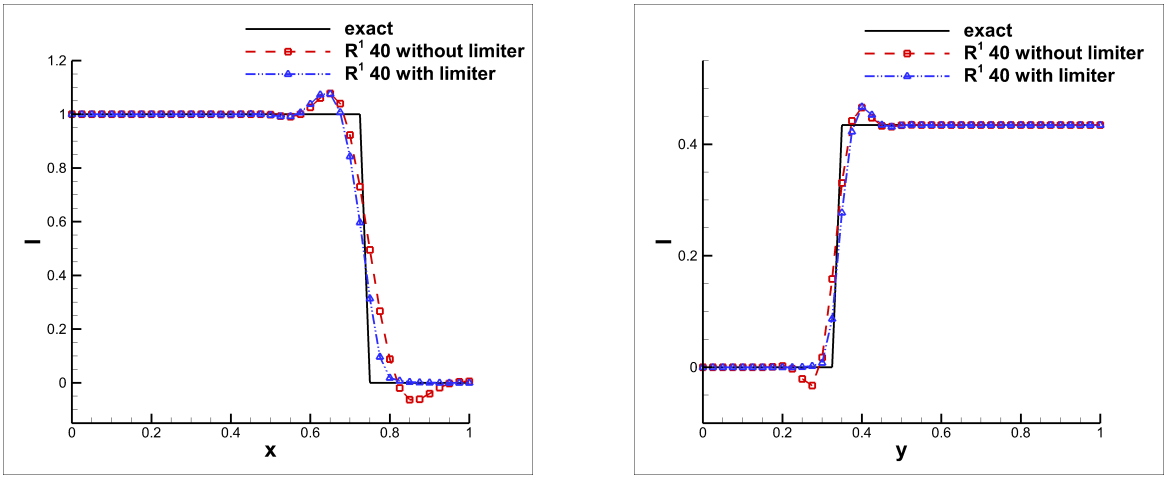

Figure 5.4: The comparison of the radiative intensity cut along the lines $y = 0.5$ and $x = 0.5$ for the transparent model simulated by the R^1 DG scheme without and with the positivity-preserving limiter on a 40×40 uniform grid. Left: $y = 0.5$; Right: $x = 0.5$.

Example 8. (The positivity-preserving test of the DG schemes on the purely absorbing model for the two-dimensional steady radiative transfer equation)

We test the scheme (2.25) on the purely absorbing model which is expressed by the equation (2.21) with $\sigma_t = 1, \sigma_s = 0$ and $q = 0$. The computational domain is $[0, 1] \times [0, 1]$. $\zeta = 0.6, \lambda = 0.4$. The boundary condition is

$$I(x, 0) = 0, \qquad I(0, y) = 1.$$

Its exact solution is as follows,

$$I(x, y) = \begin{cases} 0, & y < \frac{\lambda}{\zeta} x, \\ e^{-\frac{\sigma_t}{\zeta} x}, & \text{else.} \end{cases}$$

Figure 5.5 depicts the contour of the radiative intensity simulated by the R^1 DG scheme with the positivity-preserving limiter on a 40×40 uniform grid, where the cells in which the positivity-preserving limiter has been enacted during the computation are marked by the discrete white points. In Figure 5.6, the comparison of the radiative intensity cut along the lines $y = 0.5$ and $x = 0.5$ obtained by the R^1 DG scheme without and with the positivity-preserving limiter is presented respectively. From these figures, we can observe that the R^1 DG scheme with the positivity-preserving limiter produces positive solutions with good resolution.

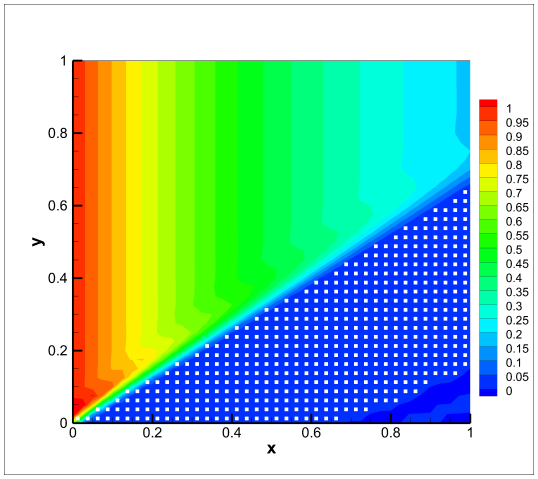

Figure 5.5: The contour of the radiative intensity for the purely absorbing model simulated by the R^1 DG scheme with the positivity-preserving limiter on a 40×40 uniform grid. The white points represent the cells where the positivity-preserving limiter has been enacted during the computation.

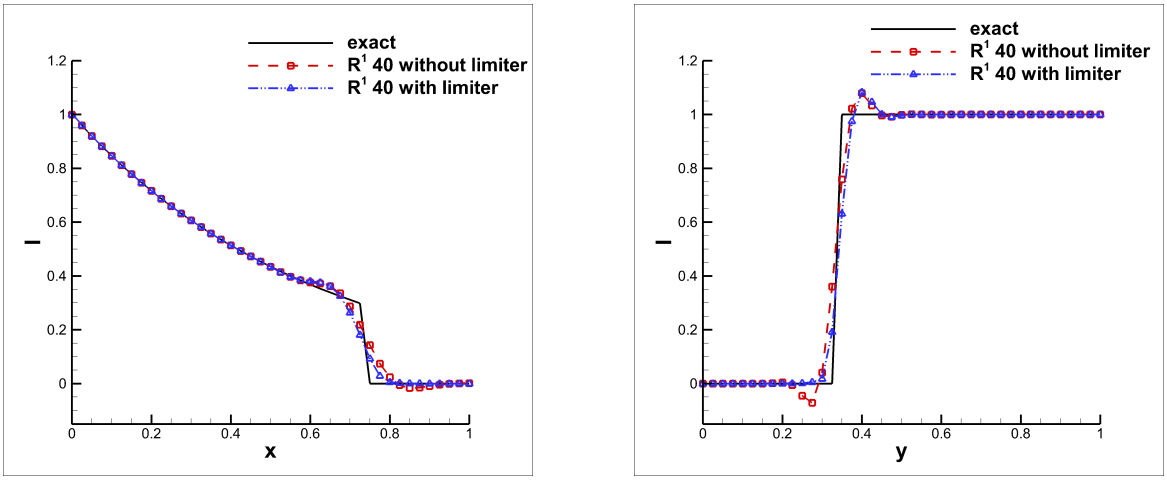

Figure 5.6: The comparison of the radiative intensity cut along the lines $y = 0.5$ and $x = 0.5$ for the purely absorbing model simulated by the R^1 DG scheme without and with the positivity-preserving limiter on a 40×40 uniform grid. Left: $y = 0.5$; Right: $x = 0.5$.

Example 9. (The positivity-preserving test of the DG schemes on the absorbing-scattering model for the two-dimensional steady radiative transfer equation)

In this problem, we test the schemes on the absorbing-scattering model described by the equation (2.21) with $\sigma_t = 1, \sigma_s = 1$ and $q = 0$. The computational domain is $[0, 1] \times [0, 1]$.

The boundary condition is set as follows,

$$\begin{aligned} &I(x,0)=0, \quad \lambda>0; && I(x,1)=0, \lambda<0; \\ &I(0,y)=1-\cos(4\pi y), \zeta>0; && I(1,y)=0, \zeta<0. \end{aligned}$$

The exact solution cannot be obtained theoretically for this problem. For comparison, we take the numerical solution by the R^1 DG scheme with the positivity-preserving limiter on a 160×160 uniform grid as a reference solution. We implement the test on a 40×40 uniform grid by using the R^1 DG scheme without and with the positivity-preserving limiter. The contour of the radiative intensity in the $(\zeta, \lambda) = (0.2578, 0.1068)$ angular direction simulated by the R^1 DG scheme with the positivity-preserving limiter is given in Figure 5.7. In the picture, the cells where the positivity-preserving limiter has taken effect during the computation are marked by discrete white points as well. Figure 5.8 shows the comparison of the radiative intensity cut along the cells near the left boundary in the $(\zeta, \lambda) = (0.3256, -0.7860)$ angular direction simulated by the R^1 DG scheme without and with the positivity-preserving limiter individually. From the figure, we notice that negative solution occurs if the R^1 DG scheme without the positivity-preserving limiter is applied, while the R^1 DG scheme with the positivity-preserving limiter can produce nonnegative solution with satisfactory resolution.

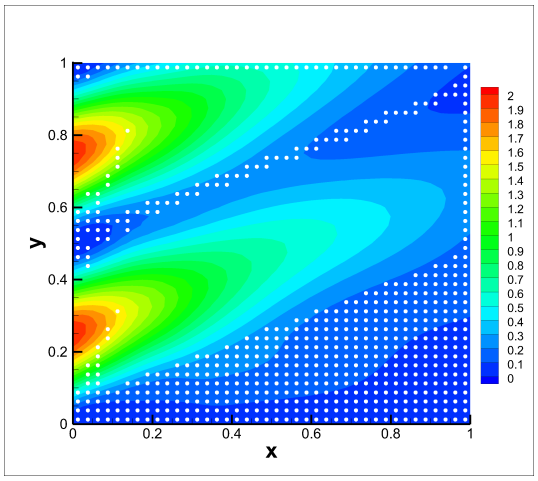

Figure 5.7: The contour of the radiative intensity for the absorbing-scattering model in the $(\zeta, \lambda) = (0.2578, 0.1068)$ angular direction simulated by the R^1 DG scheme with the positivity-preserving limiter on a 40×40 uniform grid. The white points represent the cells where the positivity-preserving limiter has been enacted during the computation.

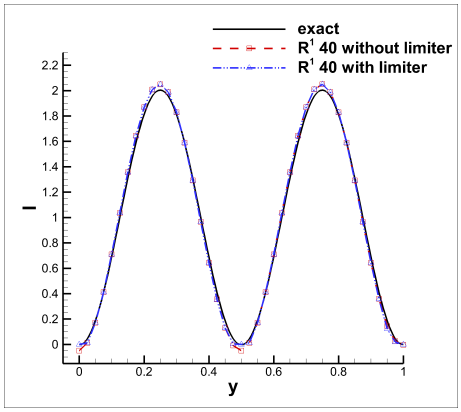

Figure 5.8: The comparison of the radiative intensity cut along the cells near the left boundary in the $(\zeta, \lambda) = (0.3256, -0.7860)$ angular direction for the absorbing-scattering model simulated by the R^1 DG scheme without and with the positivity-preserving limiter.

6 Conclusion

In this paper, we focus on the design of conservative high order positivity-preserving DG schemes for both one- and two-dimensional linear hyperbolic equations as well as the discrete ordinate radiative transfer equations. Here "conservative" refers to the fact that the cell averages from unmodulated DG solver are not altered by the positivity-preserving limiter. In the one-dimensional case, the method uses traditional DG space P^k of piecewise polynomials of degree at most k. A key result is proved that the unmodulated DG solver in this case can maintain positivity of cell averages, provided the inflow value and the source term are both positive, therefore the positivity-preserving framework in [15], namely the application of a simple scaling limiter around the cell average, can be used to obtain a high order conservative positivity-preserving DG scheme. In two-dimensions, the unmodulated DG method based either on P^k or Q^k spaces (piecewise k-th degree polynomials or piecewise tensor-product k-th degree polynomials) could generate negative cell averages. We augment the DG space with additional functions so that the positivity of cell averages from the unmodulated DG method can be restored, thereby leading to high order conservative positivity-preserving DG scheme based on these augmented DG spaces following the framework in [15]. This effort is carried out for the second order case in two-dimensional rectangular meshes as an example.

Computational results are provided to demonstrate the good performance of our DG schemes. Even though the larger augmented DG spaces involve additional computational cost, this can be reduced if an adaptive procedure is used, in which the standard P^k space is used when the computed cell average is positive, and the augmented R^k space is used only when the computed cell average from P^k is negative. In future work, we will extend the results of this paper to triangular meshes, and to higher orders of accuracy in two-dimensions. The more difficult task of generalization to the cases of variable coefficients or even nonlinear problems will also be explored.

Appendix A. The specific test function v for the augmented DG spaces

In this appendix we give explicit formulas for the specific test function v satisfying (4.1) for the augmented DG space R^1 defined in (4.5). Since we just consider the case $\alpha, \beta > 0$ in (2.7), we can simplify it as $\alpha u_x + u_y + \gamma u = f$. Besides, for the DG scheme (2.8), we also take the size of the cell $S_{i,j}$ as $\Delta x_i = \Delta y_j$, which will only effect the ratio of α and β. The formula for v is then given as

$$\begin{aligned} v(\xi,\eta) =& \frac{\Delta x_i}{\Lambda_{i,j}}\big(44\widetilde{\gamma}^3 + 3\widetilde{\gamma}^2(\alpha+1)f_1(\xi,\eta) + \widetilde{\gamma}(f_2(\xi,\eta) + 2\alpha f_3(\xi,\eta) + \alpha^2 f_4(\xi,\eta)) \\ &+ \alpha(f_5(\xi,\eta) + 2\alpha f_6(\xi,\eta) + 786\alpha^2(1-\xi)) + 786(1-\eta)\big), \end{aligned} \tag{A.1}$$

where $\Lambda_{i,j}$ reads as

$$\begin{aligned} \Lambda_{i,j} =& 4\big(393 + 393\alpha^4 + 536\widetilde{\gamma} + 310\gamma^2 + 88\widetilde{\gamma}^3 + 11\widetilde{\gamma}^4 \\ &+ 2\alpha^3(667 + 268\widetilde{\gamma}) + \alpha^2(1882 + 1481\widetilde{\gamma} + 310\widetilde{\gamma}^2) \\ &+ \alpha(1334 + 1481\widetilde{\gamma} + 583\widetilde{\gamma}^2 + 88\widetilde{\gamma}^3)\big) \end{aligned}$$

with $\widetilde{\gamma} = \gamma \Delta x_i$ and

$$\begin{aligned}
f_1(\xi,\eta) &= 106 - 5\xi^2 - 44\eta - 5\eta^2 - 20\xi\eta, \\
f_2(\xi,\eta) &= 820 - 15\xi^2 - 15\eta^2 - 558\eta - 60\xi - 60\xi\eta, \\
f_3(\xi,\eta) &= 848 + 30\xi^2 + 30\eta^2 + 120\xi\eta - 441\xi - 441\eta, \\
f_4(\xi,\eta) &= 820 - 15\xi^2 - 15\eta^2 - 558\xi - 60\eta - 60\xi\eta, \\
f_5(\xi,\eta) &= 2206 + 300\xi^2 + 300\eta^2 + 1200\xi\eta - 1158\xi - 1944\eta, \\
f_6(\xi,\eta) &= 1103 + 150\xi^2 + 150\eta^2 - 972\xi + 600\xi\eta - 579\eta.
\end{aligned} \tag{A.2}$$

We can easily prove that the functions $f_k(\xi,\eta), k = 1,\ldots,6$ are all positive when $(\xi,\eta) \in [-1,1]^2$. Hence $v(\xi,\eta)$ is positive on $S_{i,j}$.

Appendix B.

In this appendix we prove that, for the unmodulated DG scheme, all the upstream solution values at the interfaces $u^-_{i+\frac{1}{2}}$ remain positive, when the physical inflow condition and the source term are both positive and when the mesh size h is small enough. Consider the case for $\alpha > 0$ in (2.1), then (2.1) can simplified as $u_x + \gamma u = f$. By means of the similar technique utilized before, we would like to seek a special test function which satisfies

$$\int_{S_i} u(\gamma v - v' + v^-_{i+\frac{1}{2}}\delta_k(x)) = u^-_{i+\frac{1}{2}} \tag{B.1}$$

with $\delta_k(x)$ defined in (3.1). Thanks to Lemma 3.1, we obtain an ordinary differential equation for v as follows:

$$\gamma v - v' + v^-_{i+\frac{1}{2}}\delta_k(x) = \delta_k(x). \tag{B.2}$$

Once again, the fact that $v(x)$ is a polynomial with degree of k enables us to formulate $v(x)$ explicitly by the form of

$$v(x) = \begin{cases} \dfrac{\sum_{l=0}^{k} (\frac{1}{\gamma})^{l+1} \delta_k^{(l)}(x)}{1 + \sum_{l=0}^{k} (\frac{1}{\gamma})^{l+1} \delta_k^{(l)}(x_{i+\frac{1}{2}})}, & \text{if } \gamma > 0, \\ 1 \qquad\qquad\qquad\qquad\quad , & \text{if } \gamma = 0. \end{cases} \tag{B.3}$$

Obviously, $v(x)$ is positive when $\gamma = 0$. Now let us analyze the case $\gamma > 0$. We can express $\delta_k^{(l)}(x)$ more explicitly as follows

$$\delta_k^{(l)}(x) = \frac{1}{\Delta x_i}\sum_{n=0}^{k}(2n+1)p_n^{(l)}(\xi(x)) = 2^l(\frac{1}{\Delta x_i})^{l+1}\sum_{n=l}^{k}(2n+1)p_n^{(l)}(\xi). \tag{B.4}$$

Meanwhile, we can reformulate $v(x)$ as

$$\begin{aligned} v(x) &= \frac{\sum_{l=0}^{k}(\frac{1}{\gamma})^{l+1}\delta_k^{(l)}(x)}{1+\sum_{l=0}^{k}(\frac{1}{\gamma})^{l+1}\delta_k^{(l)}(x_{i+\frac{1}{2}})} = \frac{\sum_{l=0}^{k}2^l(\frac{1}{\gamma\Delta x_i})^{l+1}\sum_{n=l}^{k}(2n+1)p_n^{(l)}(\xi)}{1+\sum_{l=0}^{k}2^l(\frac{1}{\gamma\Delta x_i})^{l+1}\sum_{n=l}^{k}(2n+1)p_n^{(l)}(1)} \\ &= \frac{\sum_{l=0}^{k}2^l(\gamma\Delta x_i)^{k-l}\sum_{n=l}^{k}(2n+1)p_n^{(l)}(\xi)}{(\gamma\Delta x_i)^{k+1}+\sum_{l=0}^{k}2^l(\gamma\Delta x_i)^{k-l}\sum_{n=l}^{k}(2n+1)p_n^{(l)}(1)} \\ &= \frac{2^k(2k+1)p_k^{(k)}(\xi)+\sum_{l=0}^{k-1}2^l(\gamma\Delta x_i)^{k-l}\sum_{n=l}^{k}(2n+1)p_n^{(l)}(\xi)}{2^k(2k+1)p_k^{(k)}(1)+(\gamma\Delta x_i)^{k+1}+\sum_{l=0}^{k-1}2^l(\gamma\Delta x_i)^{k-l}\sum_{n=l}^{k}(2n+1)p_n^{(l)}(1)}. \end{aligned} \tag{B.5}$$

Here we notice that $p_k^{(k)}(\xi) = p_k^{(k)}(1)$ is a positive constant, which reads as

$$p_k^{(k)}(\xi) = p_k^{(k)}(1) = \frac{(2k)!}{2^k\cdot k!}$$

since $p_k(\xi) = \frac{1}{2^k\cdot k!}\frac{d^n}{d\xi^n}(\xi^2-1)^k$. Therefore, when the mesh size Δx_i is small enough, $v(x)$ will be positive with a value close to 1.

For smaller k, we also list the range of $\gamma\Delta x_i$ to ensure the positivity of v. Let us denote $\widetilde{\gamma} = \gamma\Delta x_i$ once again. We can write v out as a function of the variable ξ for the cases $k = 1, 2, 3, 4$ as follows:

(1) $k = 1$:

$$v(\xi) = \frac{6+\widetilde{\gamma}+3\widetilde{\gamma}\xi}{6+4\widetilde{\gamma}+\widetilde{\gamma}^2}.$$

It turns out that $v(\xi) \geq 0$ if $\widetilde{\gamma} \leq 3$.

(2) $k = 2$:

$$v(\xi) = \frac{120+12\widetilde{\gamma}(1+5\xi)+3\widetilde{\gamma}^2(-1+2\xi+5\xi^2)}{120+72\widetilde{\gamma}+18\widetilde{\gamma}^2+2\widetilde{\gamma}^3}.$$

$v(\xi)$ will be non-negative when $\widetilde{\gamma} \le 5\sqrt{\frac{2}{3}}$.

(3) $k = 3$:

$$v(\xi) = \frac{1680 + 120\widetilde{\gamma}(1+7\xi) + 30\widetilde{\gamma}^2(-1+2\xi+7\xi^2) + \widetilde{\gamma}^3(-3-15\xi+15\xi^2+35\xi^3)}{1680 + 960\widetilde{\gamma} + 240\widetilde{\gamma}^2 + 32\widetilde{\gamma}^3 + 2\widetilde{\gamma}^4}.$$

When $\widetilde{\gamma} \le 5 - \frac{5^{2/3}}{(1+\sqrt{6})^{1/3}} + \left(5(1+\sqrt{6})\right)^{1/3} \approx 5.6484$ we have $v(\xi) \ge 0$.

(4) $k = 4$:

$$\begin{aligned} v(\xi) =& \frac{5}{\Lambda}\big(24192 + 1344\widetilde{\gamma}(1+9\xi) + 336\widetilde{\gamma}^2(-1+2\xi+9\xi^2) \\ &+ 24\widetilde{\gamma}^3(-1-7\xi+7\xi^2+21\xi^3) + \widetilde{\gamma}^4(3-12\xi-42\xi^2+28\xi^3+63\xi^4)\big) \end{aligned}$$

where

$$\Lambda = 8(15120 + 8400\widetilde{\gamma} + 2100\widetilde{\gamma}^2 + 300\widetilde{\gamma}^3 + 25\widetilde{\gamma}^4 + \widetilde{\gamma}^5).$$

It is easy to prove that $v(\xi) \ge 0$ if

$$\widetilde{\gamma} \le \frac{1}{2}\left(7 - \frac{11 \cdot 7^{2/3}}{(3(81+4\sqrt{2157}))^{1/3}} + \frac{(7(81+4\sqrt{2157}))^{1/3}}{3^{2/3}}\right) \approx 4.2923.$$

References

[1] B.G. Carlson and K.D. Lathrop, Transport theory–the method of discrete ordinates, in Computing Methods in Reactor Physics, H. Greenspan, C.N. Kelber, and D. Okrent, Eds., Gordon and Breach, New York, 1968, 165-266.

[2] B. Cockburn, S. Hou and C.-W. Shu, The Runge-Kutta local projection discontinuous Galerkin finite element method for conservation laws IV: The multidimensional case, Math. Comp., 54 (1990) 545-581.

[3] B. Cockburn, S.-Y. Lin and C.-W. Shu, TVB Runge-Kutta local projection discontinuous Galerkin finite element method for conservation laws III: One dimensional systems, J. Comput. Phys., 84 (1989) 90-113.

[4] B. Cockburn and C.-W. Shu, TVB Runge-Kutta local projection discontinuous Galerkin finite element method for conservation laws II: General framework, Math. Comp., 52 (1989) 411-435.

[5] B. Cockburn and C.-W. Shu, The Runge-Kutta discontinuous Galerkin method for conservation laws V: Multidimensional systems, J. Comput. Phys., 141 (1998) 199-224.

[6] W.A. Fiveland, Discrete-ordinates solutions of the radiative transport equation for rectangular enclosures, J. Heat Transfer, 106 (1984) 699-706.

[7] K.D. Lathrop and B.G. Carlson, Discrete Ordinate Angular Quadrature of the Neutron Transport equation, Tech. Report LA-3186, Los Alamos Scientific Laboratory, 1965.

[8] P. Lesaint and P.A. Raviart, On a finite element method for solving the neutron transport equation, in Mathematical Aspects of Finite Elements in Partial Differential Equations, C.A. deBoor, Ed., Academic Press, New York, 1974, 89-145.

[9] E.E. Lewis and W.F. Miller, Jr., Computational Methods of Neutron Transport, Wiley Interscience, New York, 1984.

[10] T. Qin and C.-W. Shu, Implicit positivity-preserving high order discontinuous Galerkin methods for conservation laws, SIAM J. Sci. Comput., to appear.

[11] W.H. Reed and T.R. Hill, Triangular mesh methods for the neutron transport equation, Tech. Report LA-UR-73-479, Los Alamos Scientific Laboratory, 1973.

[12] C.-W. Shu, TVB uniformly high order schemes for conservation laws, Math. Comp., 49 (1987) 105-121.

[13] C.-W. Shu and S. Osher, Efficient implementation of essentially non-oscillatory shock-capturing schemes, J. Comput. Phys., 77 (1988) 439-471.

[14] D. Yuan, J. Cheng and C.-W. Shu, High order positivity-preserving discontinuous Galerkin methods for radiative transfer equations, SIAM. J. Sci. Comput., 38 (2016) A2987-A3019.

[15] X. Zhang and C.-W. Shu, On positivity-preserving high order discontinuous Galerkin schemes for compressible Euler equations on rectangular meshes, J. Comput. Phys., 229 (2010) 8918-8934.